Electronic Supplementary Information

In Situ Investigation of Controlled Polymorphism in Mechanochemistry at elevated Temperature

Kevin Linberg[a,b], Philipp C. Sander[a], Franziska Emmerling[a,b]*, and Adam A. L. Michalchuk[a,c]*

a. Bundesanstalt für Materialforschung und -prüfung (BAM), Richard-Willstätter-Strasse 11, 12489 Berlin (Germany)

b. Department of Chemistry, Humboldt-Universität zu Berlin, Brook-Taylor-Strasse 2,12489 Berlin (Germany)

c. School of Chemistry, University of Birmingham, Edgbaston, Birmingham, B15 2TT United Kingdom.

Content

S1 Thermodynamics Stability of Cocrystal Polymorphs

Since our measurements were performed at RT, while the literature measurement of **Form I** was performed at -163°C[1], a difference between the simulated and experimental PXRD can be observed. By taking thermal expansion into account, a good agreement of simulated and measured PXRD is achieved, Figure S1.1. For comparison with own RT measurements, the refinement diffractogram is used.

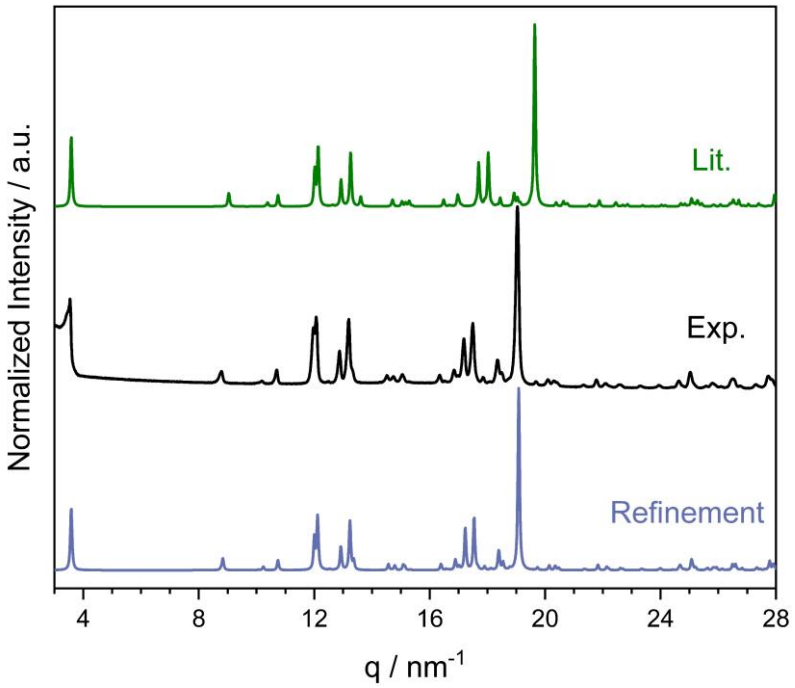

Figure S1.1| Comparison of **Form I** to the Literature (top), RT measurement (middle) and after Rietveld refinement (bottom). Since the literature diffractogram was measured at -163°C[1] and the own measurement was performed at RT, an offset can be observed. When the thermal expansion is considered, a good quality Rietveld refinement is achieved.

Various experiments were performed to determine the stability of the two polymorphs from the cocrystal NA:PA. A transformation from **Form II** to **Form I** over time can be detected, Figure S1.2. The first reflexes of **Form I** could be observed after 12 days. With the time, the amount of **Form I** increase until 45 d. No further changes in the amount of **Form I** and **Form II** can be detected.

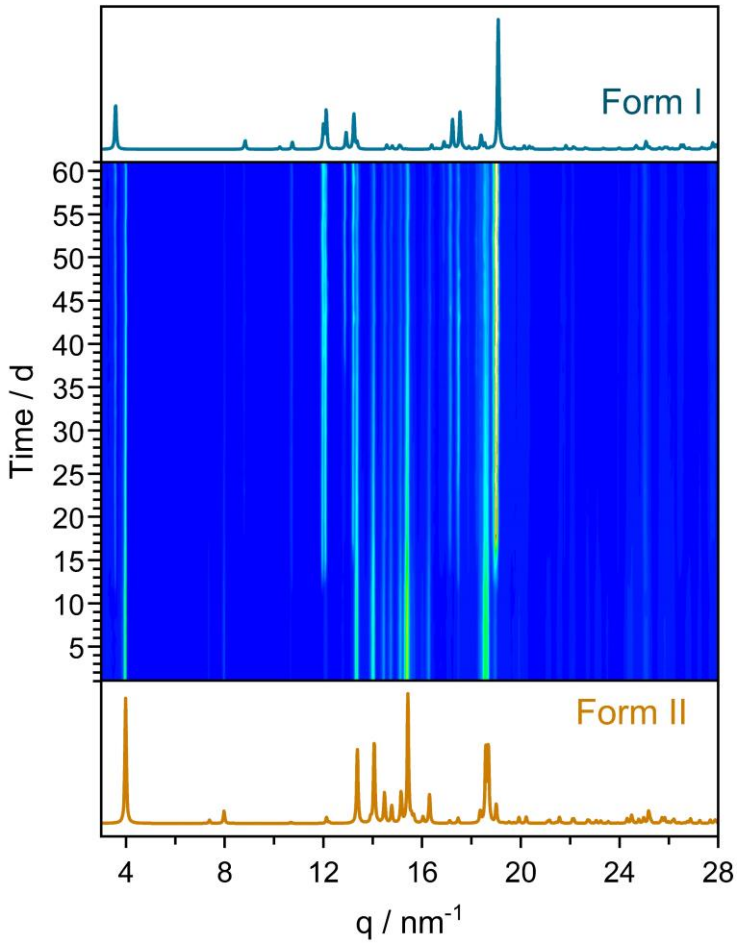

Figure S1.2| Phase transformation of **Form II** to **Form I** over time for 61 days. The diffraction patterns of **Form I** and **Form II** are shown below and above, respectively. The data were obtained *ex situ*.

To better assess the stability of **Form I** and **Form II**, slurry experiments were performed in a series of solvent: 1) a polar aprotic solvent (acetonitrile); 2) a polar protic solvent (ethanol); and 3) an apolar solvent (cyclohexane). A polymorphic mixture of 1:1 was weighed into each solvent and stirred for 72 h. All slurry experiments led to formation of **Form I**, Figure S1.3.

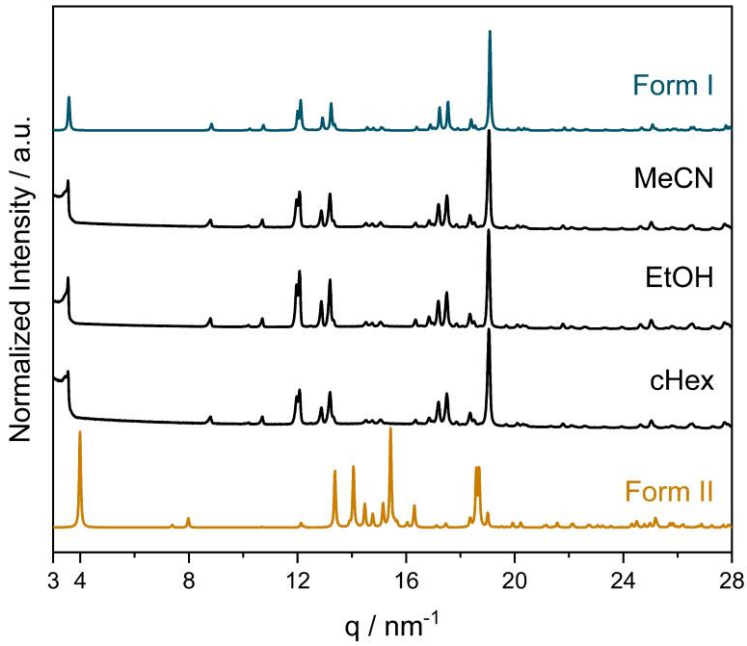

Figure S1.3| Slurry experiments with a ratio of 1:1 (**Form I**:**Form II**) performed in cyclohexane (cHex), ethanol (EtOH) and acetonitrile (MeCN). Simulated PXRD patterns of **Form I** and **Form II** are shown below and above for comparison.

Thermal analysis can provide additional information about the stability of polymorphs. Therefore, the crystalline powders of the cocrystal NA:PA were investigated by DSC and variable temperature PXRD (VT-PXRD). In the DSC experiments, both polymorphs were heated from 27°C to 147°C, Figure S1.4-S1.5. For **Form II**, a signal at 110°C can be observed, which indicates the melting point of **Form II**. **Form I** show an additional signal at 90°C and a larger signal at 110°C. The identical melting points of **Form I** and **Form II** indicate that the smaller signal at 102°C of **Form I** is a thermally induced polymorphic transformation. Both values are in good agreement with the literature values.[1] Quench cooling the melt of **Form I** and **Form II** appears to form first a glassy state, which crystallizes at 345 K to obtain the **Form II** modification. **Form II** could be obtained after quench cooling at different heating rates (1, 5, and 10 °C.min^{-1}). This suggests that melting consistently favors **Form II**. The phase transformation from **Form I** to **Form II** could also be observed using VT-PXRD, Figure S1.6. When **Form I** is heated to 90°C, the first reflections of **Form II** can be detected. **Form II** can be obtained purely at 95°C. This also agrees very well with the literature values where slurry experiments were performed at 90°C.[1]

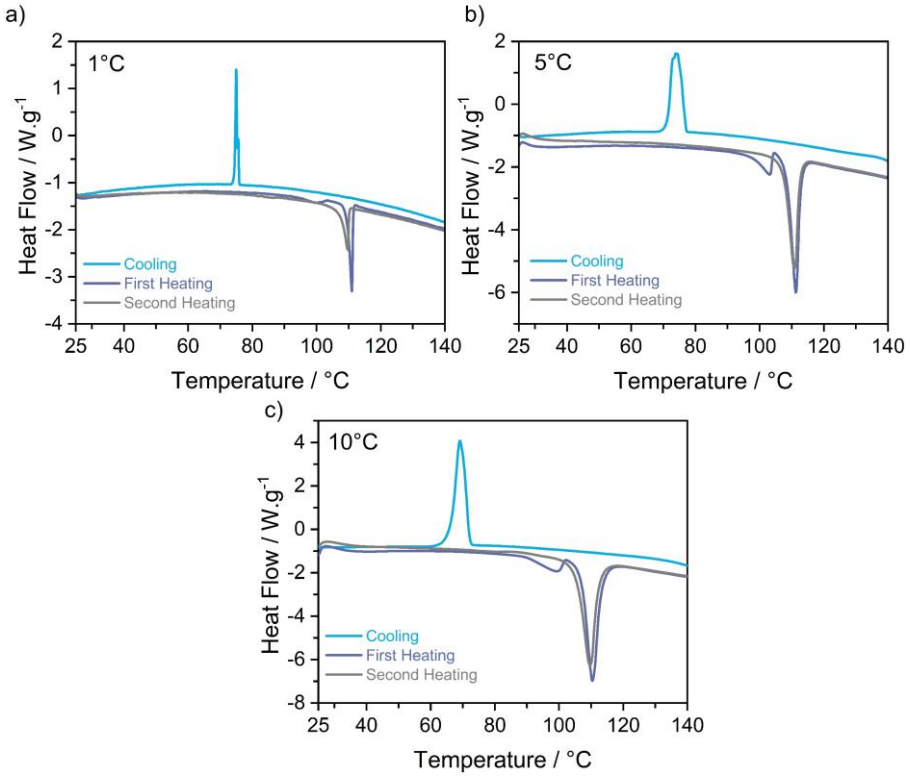

Figure S1.4| DSC measurements of **Form I** with a heat rate of a) 1 b) 5 and c) 10 °C.min^{-1}. Powder of **Form I** was heated up to 140°C (purple), cooled down to 57°C (blue) and heated again to 140°C (grey).

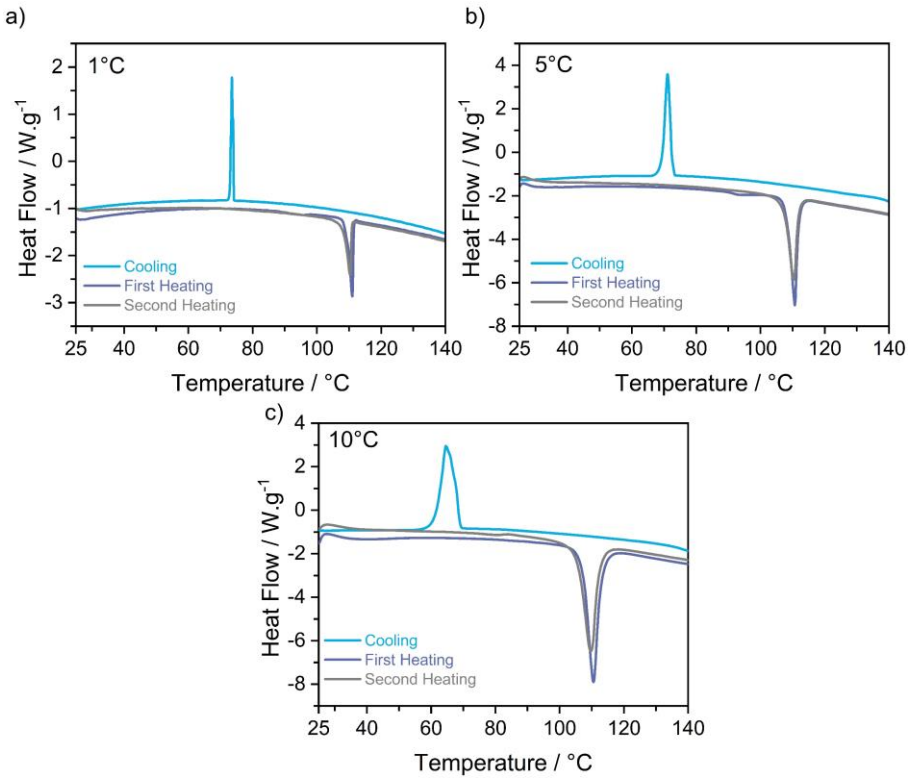

Figure S1.5| DSC measurements of **Form II** with a heat rate of a) 1 b) 5 and c) 10 °C.min^{-1}. Powder of **Form II** was heated up to 140°C (purple), cooled down to 25°C (blue) and heated again to 140°C (grey).

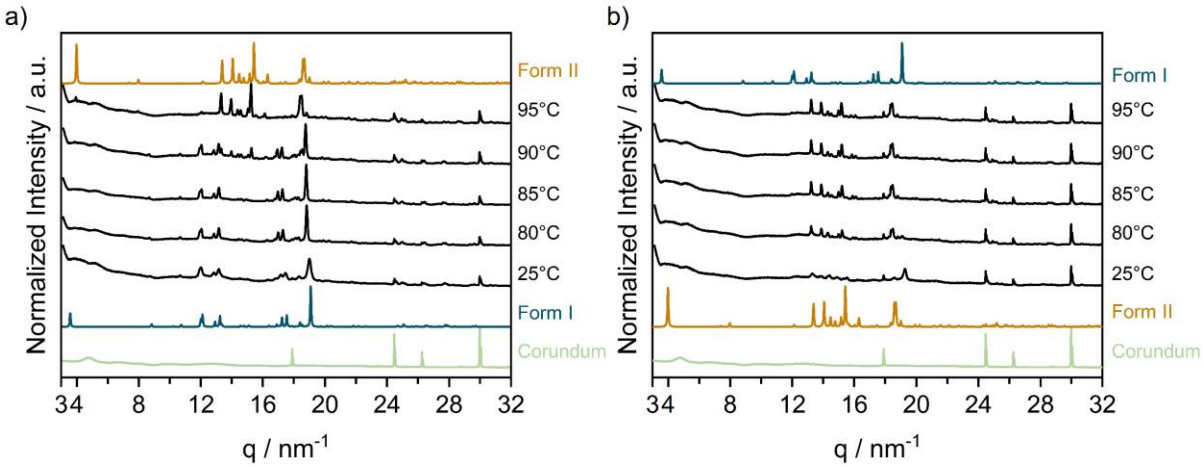

Figure S1.6| PXRD profiles from a) **Form I** and b) **Form II** at different temperatures (25 to 90°C). PXRD patterns for **Form I**, **Form II** and the empty jar are given for comparison.

The simulations of the Helmholtz free energy in Figure 2d include the temperature-dependent entropic term obtained from phonon simulations performed at k=Γ. This is a significant approximation, as it omits any inclusion of phonon dispersion. To measure the effect of this approximation, we also calculated the entropic correction on a 2 x 2 x 2 Monkhorst-Pack grid, Figure 1.7a. Changing the k-point has little effect on **Form II**, but there was an increase in the entropy of **Form I**. However, recalculating the Helmholtz free energy on this larger grid size made only small difference to the relative energies for **Form I** than **Form II**, Figure S1.7b.

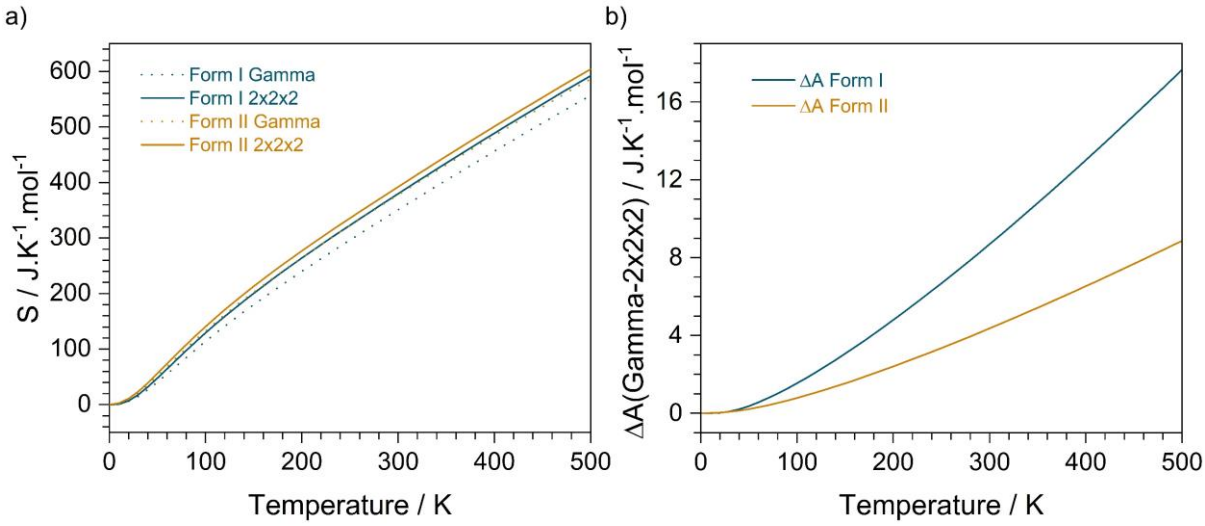

Figure S1.7| a) Comparison of the entropy of **Form I** (blue) and **Form II** (orange) calculated at the Γ-point in reciprocal space (dashed line) and over a 2x2x2 k-point grid (solid line). b) Difference in the simulated Helmholtz free energy at the gamma point and in the 2x2x2 k-point grid for **Form I** (blue) and **Form II** (orange) with the equation ΔA = A(Gamma)-A(2x2x2).

S2 Ball Milling

Our ball milling experiments were performed at three different frequencies (50, 35, and 20 Hz) and one stainless steel ball of varying sizes (10, 8, and 6 mm) was added, Figure S2.1. When ball milling a stoichiometric mixture of NA + PA led to the formation of **Form I** after 30 min at a frequency of 50 Hz and a ball size of 10 mm. No further changes in the PXRD pattern were detected with further ball milling for up to 24 h. In addition, with all other milling conditions, pure **Form I** could be obtained, whereby with lower energy input, more milling time is required. With a frequency of 20 Hz and a ball size of 6 mm, pure **Form I** could be obtained after 24 h. No reflections of **Form II** could be observed when ball milling at ambient conditions via *ex situ* measurements.

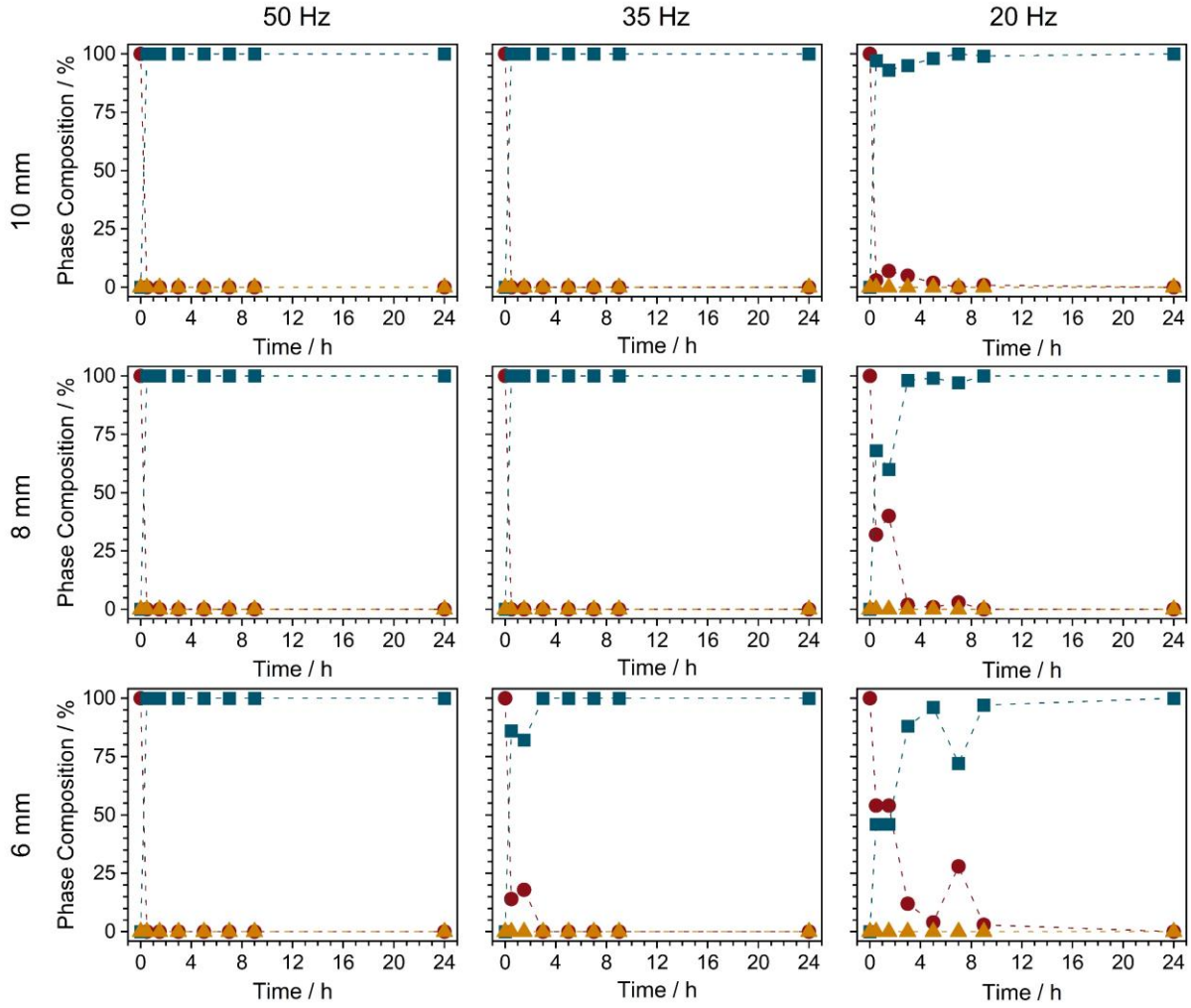

Figure S2.1| The Phase composition of the ball milling process at ambient temperature of the cocrystal NA:PA for 50 Hz (left), 35 Hz (middle), and 20 Hz (right) with different ball sizes, 10 mm (top), 8 mm (middle), and 6 mm (bottom). Data are shown for sum of the starting materials NA and PA (red circle), **Form I** (blue square), and **Form II** (orange triangle). The data were obtained *ex situ*.

Using time-resolved *in situ* (TRIS) PXRD, we investigated the time evolution of the ball milling process more closely. The experiments were performed at three different frequencies (50, 35, and 20 Hz) with a ball size of 10 mm (Figure 3, description in the main text) and using a frequency of 50 Hz with ball sizes of 8 and 6 mm, Figure S2.2. When a stoichiometric mixture of NA + PA was ball milled with a ball size of 8 mm, the reflections of **Form II** were observed after 30 s of milling (see Bragg reflections at q = 3.95 and 18.59 nm^{-1}). After 2.5 min of ball milling, reflections of **Form I** were detected (see Bragg reflections at q = 3.48 and 18.92 nm^{-1}). With continued milling, the reflections of **Form II** lost intensity and could no longer be observed anymore after 9 min of milling. Pure **Form II** was obtained after 12 min of ball milling. A similar ball milling reaction from NA+PA was observed for a ball size of 6 mm.

Under all investigated ball milling conditions, **Form II** can be observed as an intermediate during the ball milling process, but it is not sufficiently stable and will transform into **Form I** with prolonged milling time.

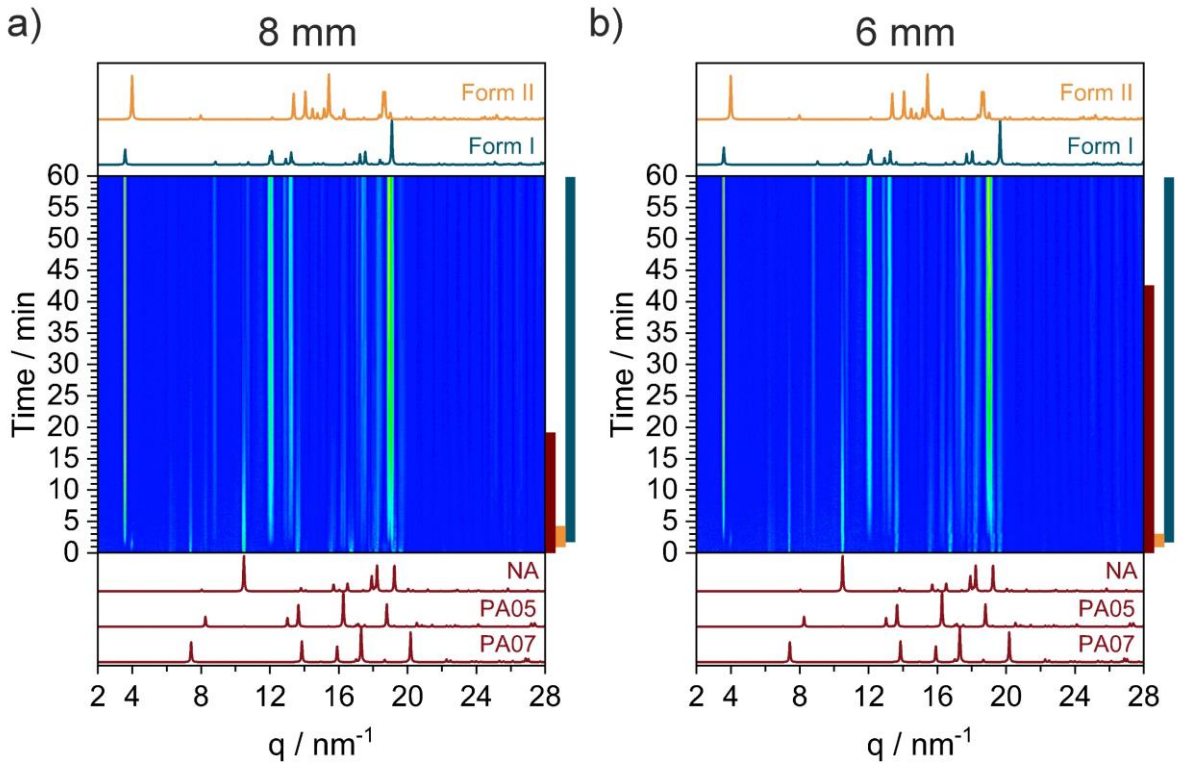

Figure S2.2| Time-resolved *in situ* (TRIS) PXRD measurements at ambient temperature with a frequency of 50 Hz and ball sizes of a: 8 mm and b: 6 mm. The colors mark the phases present in each step (starting materials: red, **Form I**: blue, and **Form II**: orange).

A polymorphic transformation from **Form I** to **Form II** occurs upon heating the powder at 90°C. By combining the ball milling energy with the milling temperature, this transition point should decrease. As a first test, we investigated cocrystal formation via ball milling with the highest energy input (50 Hz, 10 mm) at different milling temperatures (45, 55, and 65°C), Figure S2.3. Under this milling condition, milling a stoichiometric mixture of NA + PA led to pure **Form II** at 65°C without any sign of **Form I** for up to 30 min of ball milling. A Phase transformation from **Form II** to **Form I** can be observed in the temperature range of 45-55°C, but with increasing temperature reflections of **Form II** can be observed for a longer time.

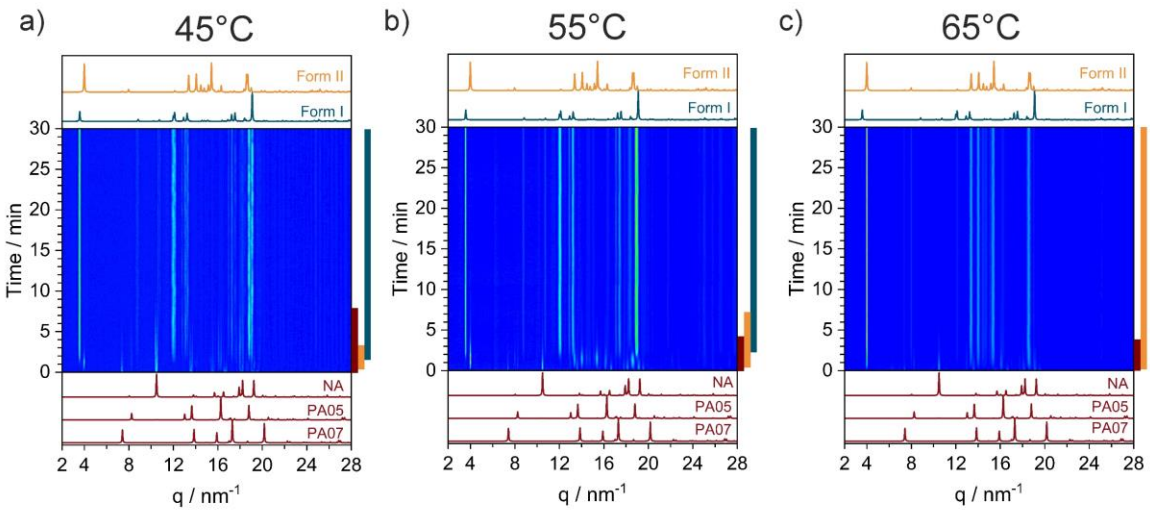

Figure S2.3| Time-resolved *in situ* (TRIS) PXRD measurements at a frequency of 50 Hz and a ball size of 10 mm at different temperatures, a) 45°C, b) 55°C, and c) 65°C. The colors mark the phases present in each step (starting materials: red, **Form I**: blue and **Form II**: orange).

An energy barrier must be overcome for any physical or chemical process. To investigate whether the energy input plays a role in stabilizing **Form II**, ball milling experiments were performed at 65°C with three different frequencies (50, 35, and 20 Hz) and a ball size of 10 mm. Ball milling at a frequency of 50 Hz led to pure **Form II** after 2 min, with no further changes in the PXRD profiles, Figure S2.4a. Similar behavior was observed at a frequency of 35 Hz, whereas pure **Form II** was obtained after 14 min of ball milling. A temperature of 65°C with a frequency of 20 Hz led to polymorph transformation from **Form II** to **Form I** after 33 min of ball milling. Pure **Form I** was obtained after 57 min of ball milling. This result indicates that energy input is crucial for the stabilization of **Form II** during ball milling.

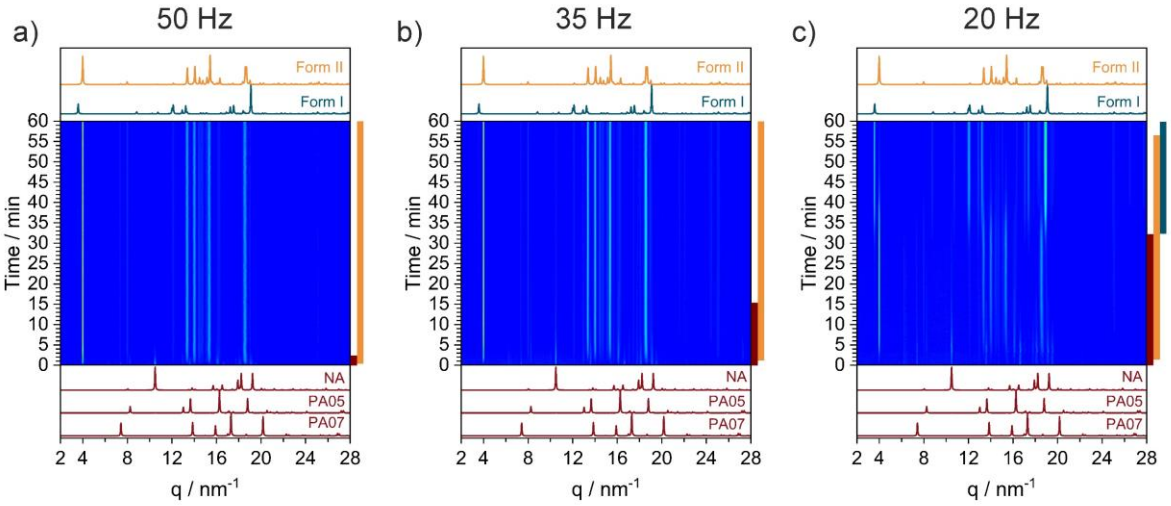

Figure S2.4| Time-resolved *in situ* (TRIS) PXRD measurements at a temperature of 65°C with a ball size of 10 mm and a frequency of a: 50 Hz, b: 35 Hz, and c: 20 Hz. The colors mark the phases present in each step (starting materials: red, **Form I**: blue and **Form II**: orange).

Therefore, we attempted to determine the extent to which such combinations are possible by investigating at temperatures of 55, 65, 75, 80 and 85°C with three different frequencies (50, 35, and 20 Hz) and one stainless steel jar with varying sizes (10, 8, and 6 mm), Figure S2.4-2.5. *Ex situ* investigation of the ball milling experiments at these different temperatures showed a strong

dependence between the energy input, temperature, and observation and lifetime of **Form II**, Figure 4 and Figure S2.5-2.6.

By reducing the ball size to 8 mm (Figure S2.5), with a frequency of 50 Hz, **Form II** can already be observed at a temperature of 65°C. By reducing the frequency to 35 Hz, the first reflections of **Form II** can be observed at a temperature of 75°C. At the lowest investiagted frequency (20 Hz), reflections of **Form II** can be observed at 80°C. After 2 h of ball milling, **Form II** gradually changes to **Form I** (**Form I**: 25 %, **Form II**: 75 %). It is similar at 85°C, whereby after 2 h only traces of **Form I** are visible (**Form I**: 7 %, **Form II**: 93 %).

Reducing the ball size to 6 mm, reflections of **Form II** were observed at a temperature of 65°C with a frequency of 50 Hz. But **Form II** was not sufficient and was not detectable after 2 h of ball milling. Upon increasing the temperature to 75°C, reflections of **Form I** were observed after 2 h of ball milling. Pure **Form II** powder with a ball size of 6 mm could be observed at a temperature of 85°C.

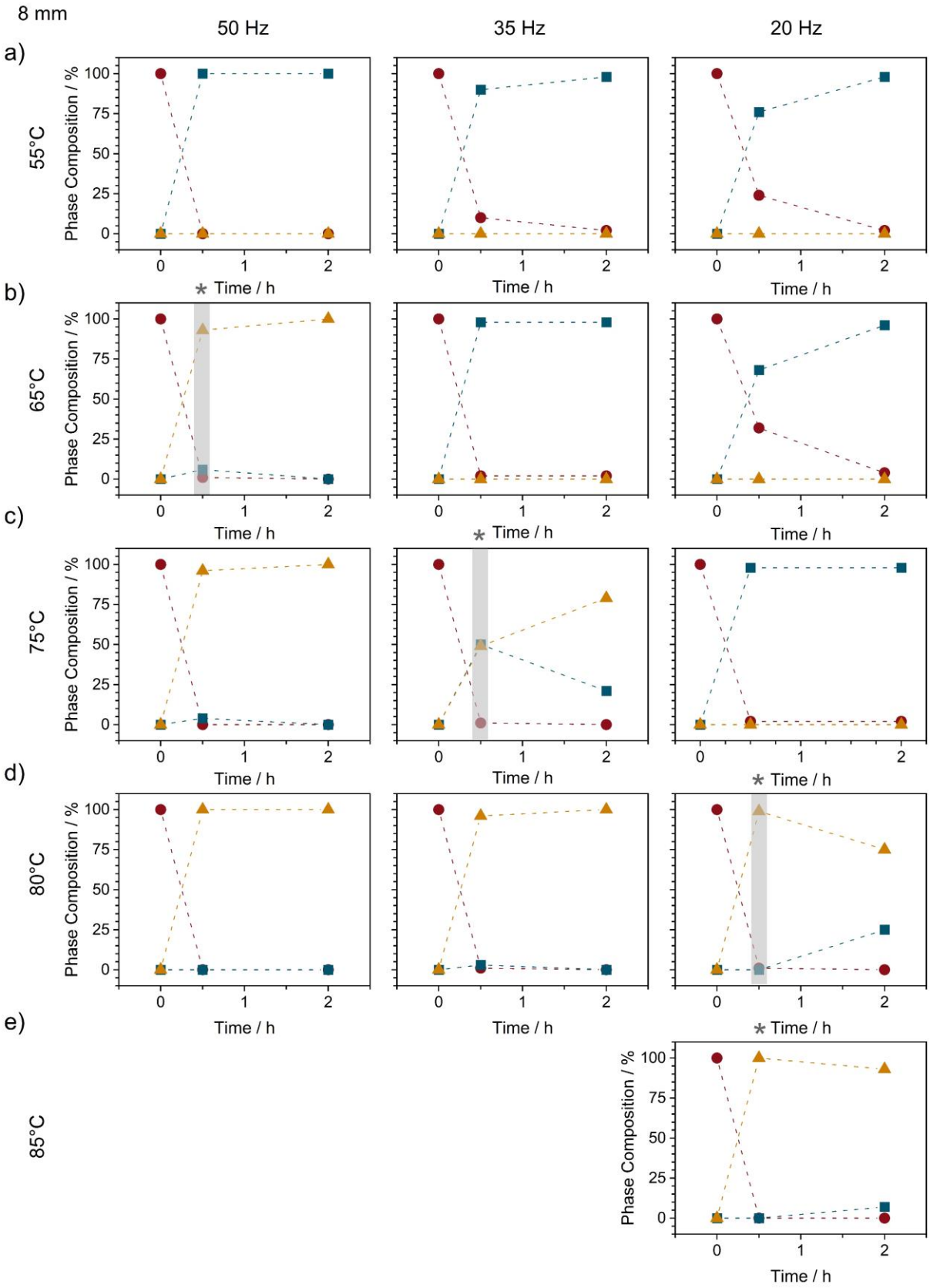

Figure S2.5| The Phase composition of the milling experiments of NA + PA for the indicated period with a ball size of 8 mm and three different frequencies (left:50 Hz, middle: 35 Hz, and right: 20 Hz) at different milling temperatures, 55 (a), 65 (b), 75 (c), 80 (d) and 85°C (e). Data are shown for the sum of the starting materials (red circles), **Form I** (blue squares), and **Form II** (orange triangles). The first observation of **Form II** for each frequency is labeled with a grey bar and star above the graph. Due to the fact that the jar breaks at 85°C with a frequency of 50 and 35 Hz, no measurements were possible. The data were obtained *ex situ*.

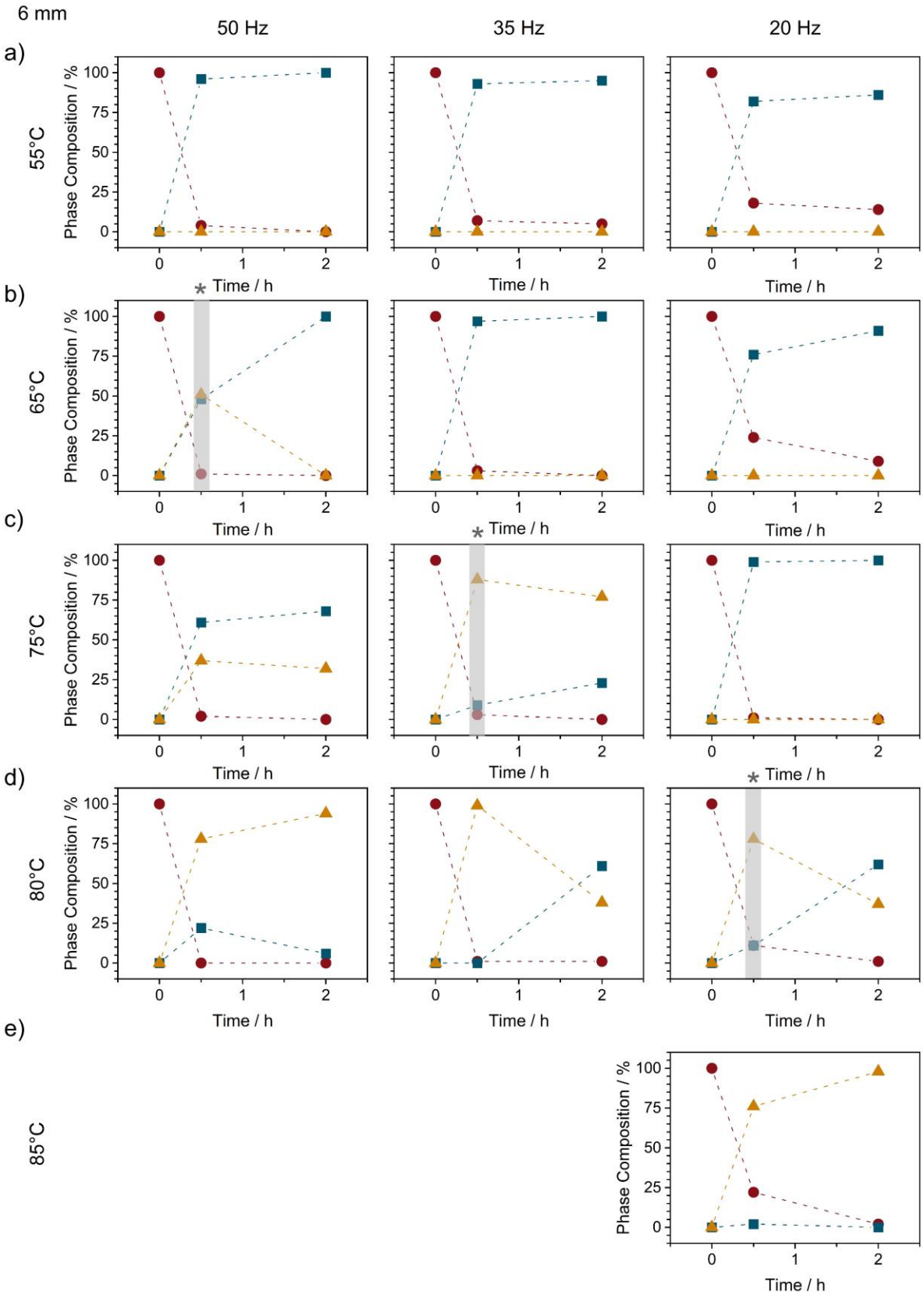

Figure S2.6| The Phase composition of the milling experiments of NA + PA for the indicated period with a ball size of 6 mm and three different frequencies (left:50 Hz, middle: 35 Hz, and right: 20 Hz) at different milling temperatures, 55 (a), 65 (b), 75 (c), 80 (d) and 85°C (e). Data are shown for the sum of the starting materials (red circles), **Form I** (blue squares), and **Form II** (orange triangles). The first observation of **Form II** for each frequency is labeled with a grey bar and star above the graph. Due to the fact that the jar breaks at 85°C with a frequency of 50 and 35 Hz, no measurements were possible. The data were obtained *ex situ*.

Ball milling at different temperatures can be used to control the interconversion of polymorphic forms under milling conditions. Ball milling experiments have also been performed to see if this is also the true for the pure polymorphs. Ball milling experiments were performed at a frequency of 50 Hz and a ball size of 10 mm. When **Form II** is milled at ambient temperature (Figure S2.7a), it converts to **Form I** much faster than when aged over time. Pure Form II can be obtained after 7 min of ball milling. Moreover, ball milling **Form I** at temperature of 55 and 65°C did not transform to **Form II** for up to 1 h of ball milling, Figure S2.7b and c. Ball milling at 75°C led to polymorphic transformation, Figure S2.7d. The first reflections of **Form II** were observed after 3 min of ball milling. Complete transformation to **Form II** was detected after 25 min of ball milling. The direct polymorph conversion from **Form I** to **Form II** requires a higher temperature than the formation of **Form II** from the starting materials (65°C).

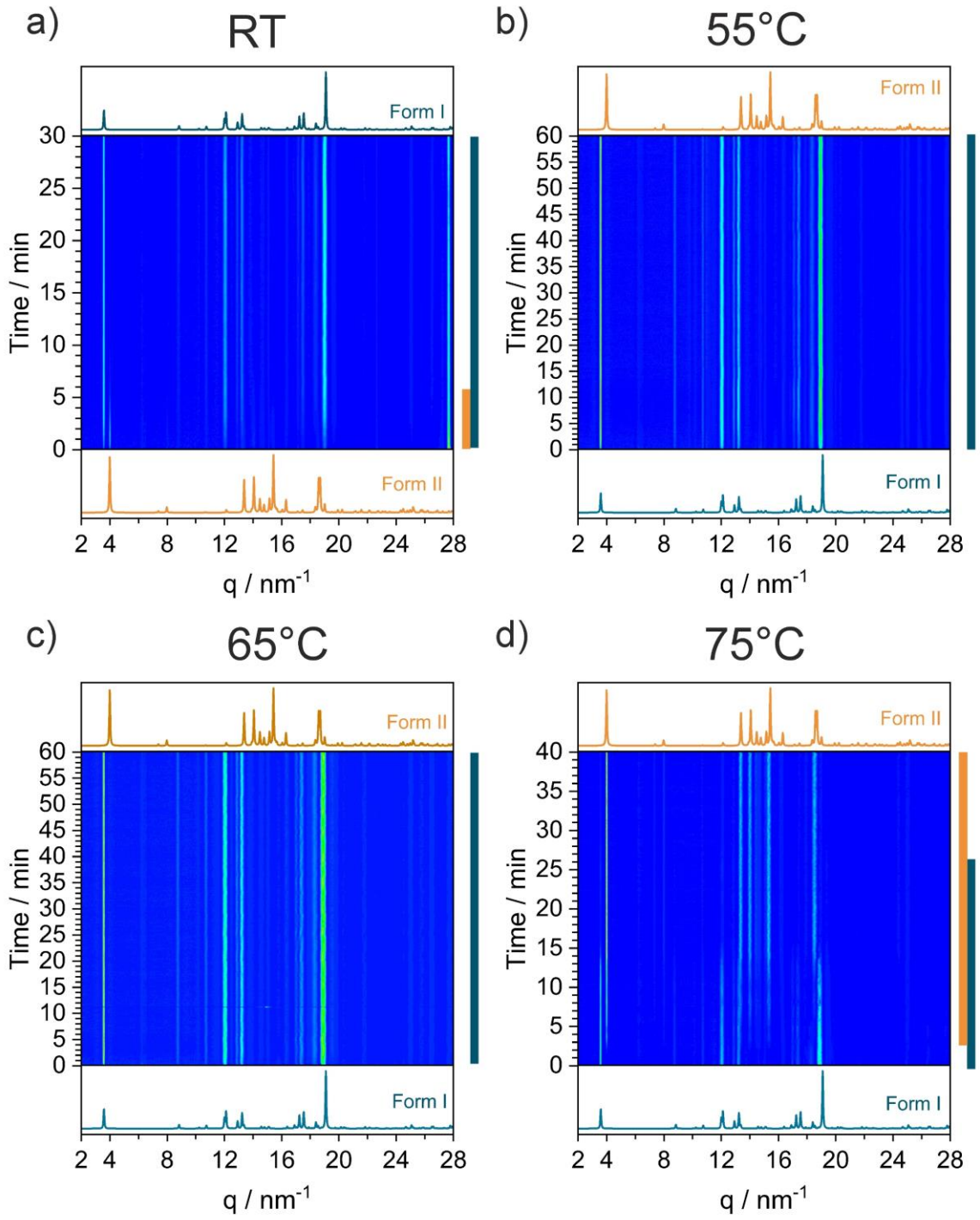

Figure S2.7| a) Time-resolved *in situ* (TRIS) PXRD measurements at a frequency of 50 Hz and a ball size of 10 mm at ambient temperatures for **Form II**. b) TRIS PXRD measurements at a frequency of 50 Hz and a ball size of 10 mm for **Form I** at different temperature, b) 55°C, c) 65°C. and d) 75°C. The colors mark the phases present in each step (starting materials: red, **Form I**: blue and **Form II**: orange).

Ex situ, a polymorph conversion from **Form I** to **Form II** was also observed at a temperature of 75°C, Figure S2.8a. The experiments were performed at a frequency of 50 Hz and a ball size of 10 mm. **Form II** was stable under these conditions up to 9 h of ball milling. However, one of the four experiments at 9 h of ball milling also resulted in reflections of **Form I**. This may be because **Form I** powder being stuck in the jar and not reacting during the ball milling experiment. As **Form II** remained

stable after repeated the ball milling experiments at 9 h, we assume that **Form II** is the stable phase under these milling conditions.

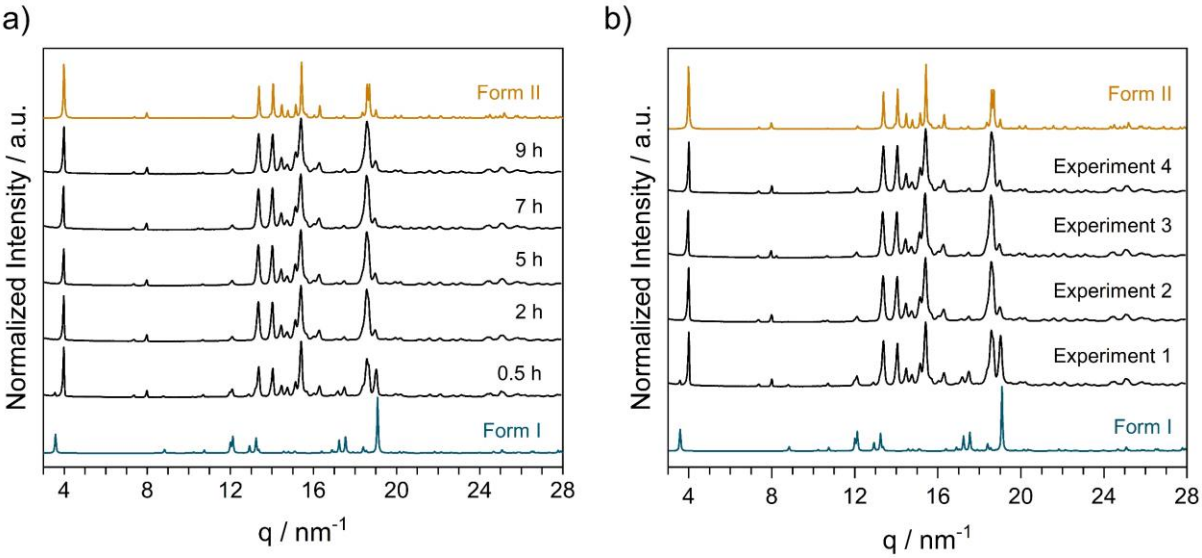

Figure S2.8| Results of the milling experiments at a temperature of 75°C for ball milling **Form I** with a milling ball of 10 mm and a frequency of 50 Hz. a) Ball milling for 0.5, 2, 5, 7, and 9 h. b) Repeat ball milling at 9 h. The data were obtained *ex situ*.

S3 Rietveld Refinement of Mechanochemically Prepared Powders

Rietveld refinement was performed for all mechanochemically produced powders for phase analysis. This allows the characterization of the phase composition of the powder. The table with the Phase composition for each milling condition and the crystallite size of **Form II** or **Form I** can be found under the respective Rietveld refinement Figure (ambient temperature: Figure (S3.1-S3.9) and Table (S3.1-S3.9), at 55°C Figure (S3.10-S3.12) and Table (S3.10-S3.12), at 65°C Figure (S3.13-S3.15) and Table (S3.13-S3.15), at 75°C Figure (S3.16-S3.18) and Table (S3.16-S3.18), at 80°C Figure (S3.19-S3.21) and Table (S3.19-S3.21), and at 85°C Figure (S3.22) and Table (S3.22).

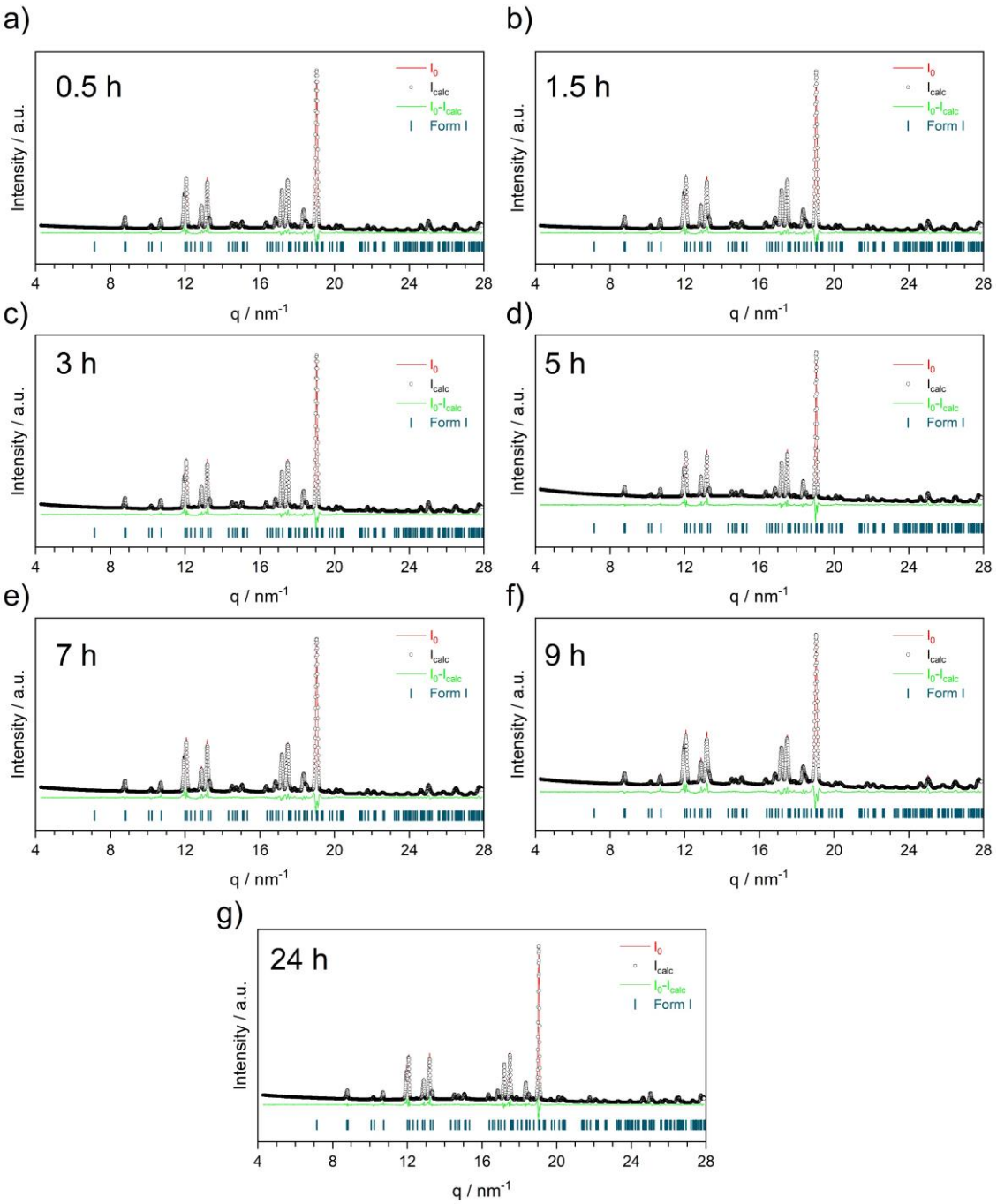

Figure S3.1| Results of the phase analyses for the mechanochemical synthesis of the cocrystal NA:PA with a ball size of 10 mm and a frequency of 50 Hz at ambient temperature: a) at a ball milling time of 0.5 h (R_{wp} = 6.517); b) at a ball milling time of 1.5 h (R_{wp} = 7.429); c) at a ball milling time of 3 h (R_{wp} = 6.210); d) at a ball milling time of 5 h (R_{wp} = 5.622), e) at a ball milling time of 7 h (R_{wp} = 7.060), f) at a ball milling time of 9 h (R_{wp} = 7.180) and g) at a ball milling time of 24 h (R_{wp} = 6.069).

Table S3.1| Results of the Rietveld quantitative phase analyses for the mechanochemical synthesis of the cocrystal NA:PA using a 10 mm milling ball and a frequency of 50 Hz at ambient temperature. The weighted *R*-factor (R_{wp}) is given alongside the crystal sizes (CS) obtained from the Scherrer equation.

time	Reagents /%	Form I / %	Form II / %	R_{wp}	CS (Form I) / nm	CS (Form II) / nm
0.5 h	0	100	0	6.517	139 ± 5	-
1.5 h	0	100	0	7.429	155 ± 7	-
3 h	0	100	0	6.210	165 ± 7	-
5 h	0	100	0	5.622	228 ± 17	-
7 h	0	100	0	7.060	145 ± 7	-
9 h	0	100	0	7.180	99 ± 3	-
24 h	0	100	0	6.069	162 ± 4	-

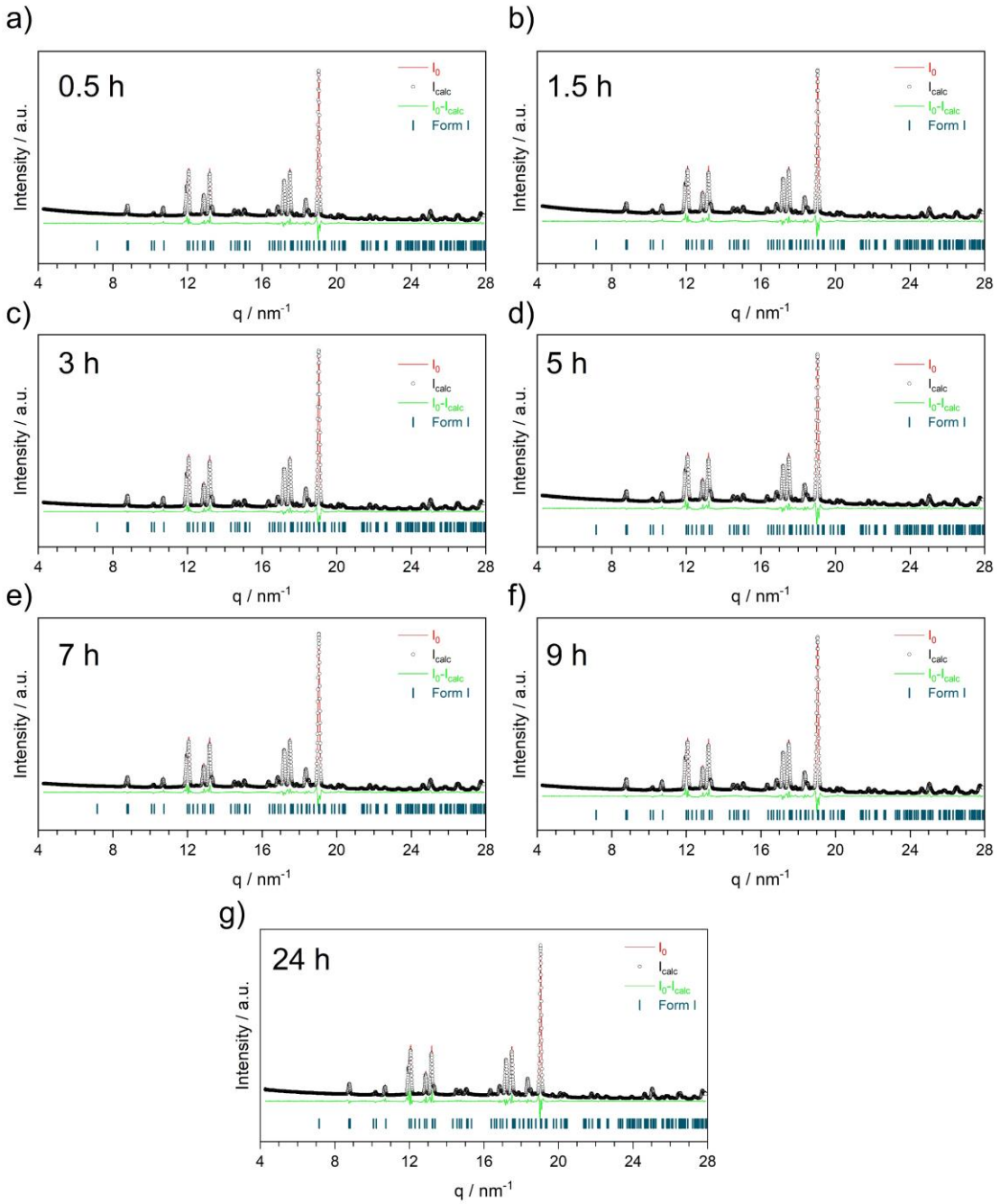

Figure S3.2| Results of the phase analyses for the mechanochemical synthesis of the cocrystal NA:PA with a ball size of 8 mm and a frequency of 50 Hz at ambient temperature: a) at a ball milling time of 0.5 h (R_{wp} = 5.832); b) at a ball milling time of 1.5 h (R_{wp} = 6.034); c) at a ball milling time of 3 h (R_{wp} = 6.753); d) at a ball milling time of 5 h (R_{wp} = 6.780), e) at a ball milling time of 7 h (R_{wp} = 6.889), f) at a ball milling time of 9 h (R_{wp} = 6.827) and g) at a ball milling time of 24 h (R_{wp} = 7.559).

Table S3.2| Results of the Rietveld quantitative phase analyses for the mechanochemical synthesis of the cocrystal NA:PA using an 8 mm milling ball and a frequency of 50 Hz at ambient temperature. The weighted *R*-factor (R_{wp}) is given alongside the crystal sizes (CS) obtained from the Scherrer equation.

time	Reagents /%	Form I / %	Form II / %	R_{wp}	CS (Form I) / nm	CS (Form II) / nm
0.5 h	0	100	0	5.832	180 ± 9	-
1.5 h	0	100	0	6.034	114 ± 3	-
3 h	0	100	0	6.753	143 ± 6	-
5 h	0	100	0	6.780	105 ± 3	-
7 h	0	100	0	6.889	103 ± 2	-
9 h	0	100	0	6.827	136 ± 6	-
24 h	0	100	0	7.559	74 ± 1	-

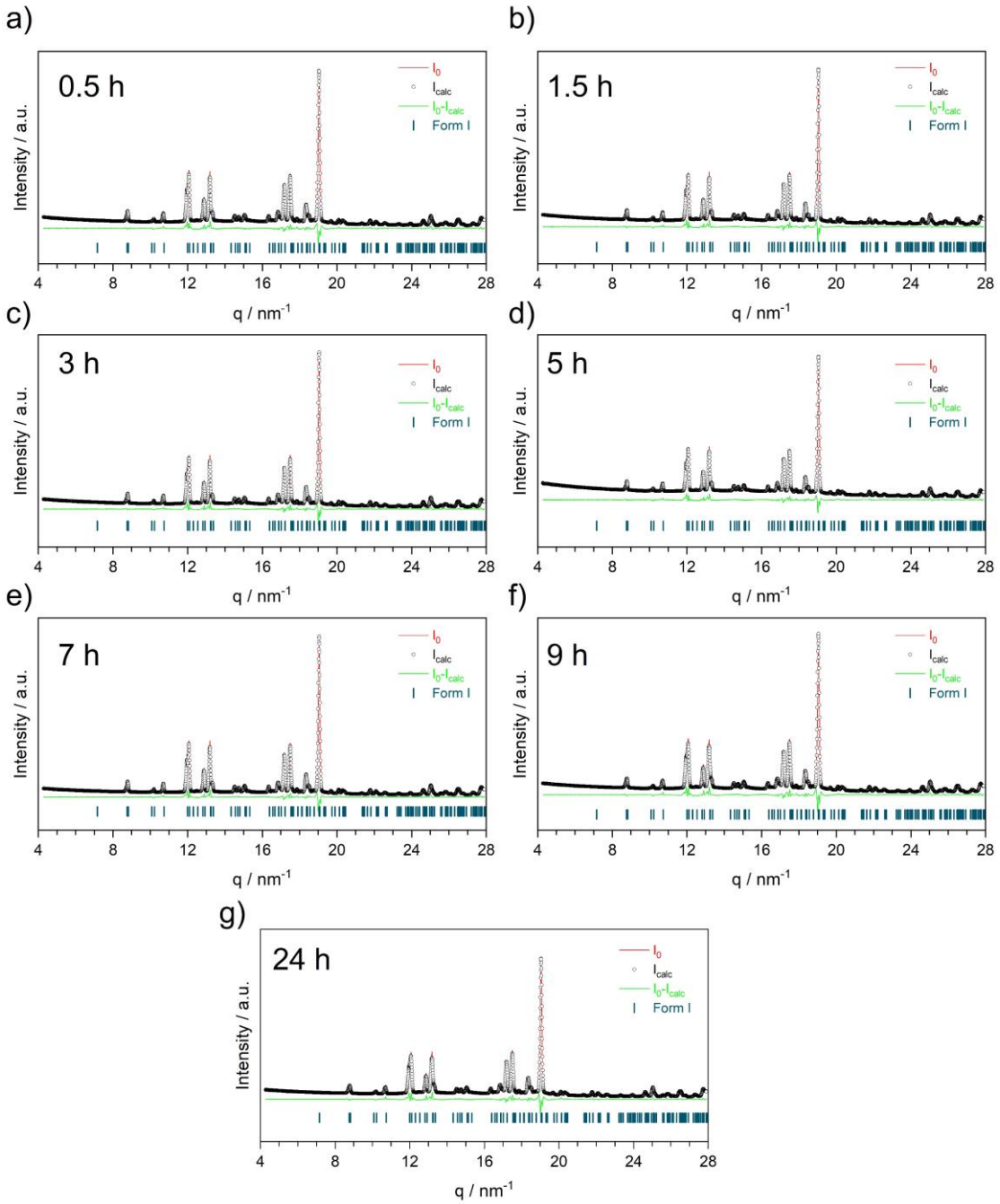

Figure S3.3| Results of the phase analyses for the mechanochemical synthesis of the cocrystal NA:PA with a ball size of 6 mm and a frequency of 50 Hz at ambient temperature: a) at a ball milling time of 0.5 h (R_{wp} = 6.226); b) at a ball milling time of 1.5 h (R_{wp} = 5.964); c) at a ball milling time of 3 h (R_{wp} = 6.575); d) at a ball milling time of 5 h (R_{wp} = 4.794), e) at a ball milling time of 7 h (R_{wp} = 6.993), f) at a ball milling time of 9 h (R_{wp} = 6.589) and g) at a ball milling time of 24 h (R_{wp} = 6.634).

Table S3.3| Results of the Rietveld quantitative phase analyses for the mechanochemical synthesis of the cocrystal NA:PA using a 6 mm milling ball and a frequency of 50 Hz at ambient temperature. The weighted *R*-factor (R_{wp}) is given alongside the crystal sizes (CS) obtained from the Scherrer equation.

time	Reagents /%	Form I / %	Form II / %	R_{wp}	CS (Form I) / nm	CS (Form II) / nm
0.5 h	0	100	0	6.226	178 ± 10	-
1.5 h	0	100	0	5.964	151 ± 5	-
3 h	0	100	0	6.575	181 ± 8	-
5 h	0	100	0	4.794	224 ± 16	-
7 h	0	100	0	6.993	89 ± 2	-
9 h	0	100	0	6.589	194 ± 10	-
24 h	0	100	0	6.634	78 ± 1	-

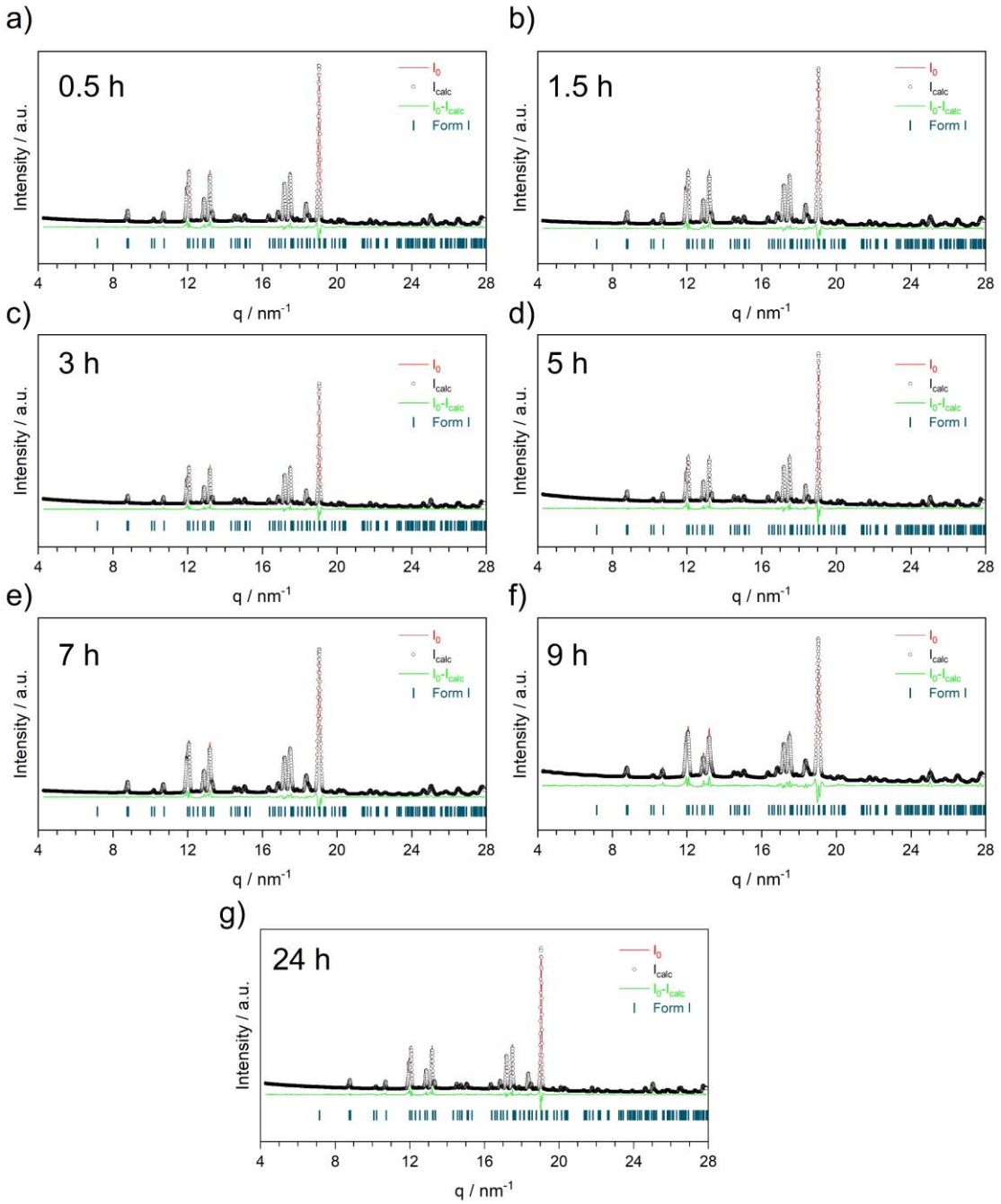

Figure S3.4| Results of the phase analyses for the mechanochemical synthesis of the cocrystal NA:PA with a ball size of 10 mm and a frequency of 35 Hz at ambient temperature: a) at a ball milling time of 0.5 h (R_{wp} = 6.277); b) at a ball milling time of 1.5 h (R_{wp} = 6.821); c) at a ball milling time of 3 h (R_{wp} = 5.663); d) at a ball milling time of 5 h (R_{wp} = 5.690), e) at a ball milling time of 7 h (R_{wp} = 7.256), f) at a ball milling time of 9 h (R_{wp} = 7.445) and e) at a ball milling time of 24 h (R_{wp} = 5.808).

Table S3.4| Results of the Rietveld quantitative phase analyses for the mechanochemical synthesis of the cocrystal NA:PA using a 10 mm milling ball and a frequency of 35 Hz at ambient temperature. The weighted *R*-factor (R_{wp}) is given alongside the crystal sizes (CS) obtained from the Scherrer equation.

time	Reagents /%	Form I / %	Form II / %	R_{wp}	CS (Form I) / nm	CS (Form II) / nm
0.5 h	0	100	0	6.277	228 ± 18	-
1.5 h	0	100	0	6.821	184 ± 12	-
3 h	0	100	0	5.663	232 ± 16	-
5 h	0	100	0	5.690	210 ± 11	-
7 h	0	100	0	7.256	142 ± 7	-
9 h	0	100	0	7.445	68 ± 2	-
24 h	0	100	0	5.808	210 ± 10	-

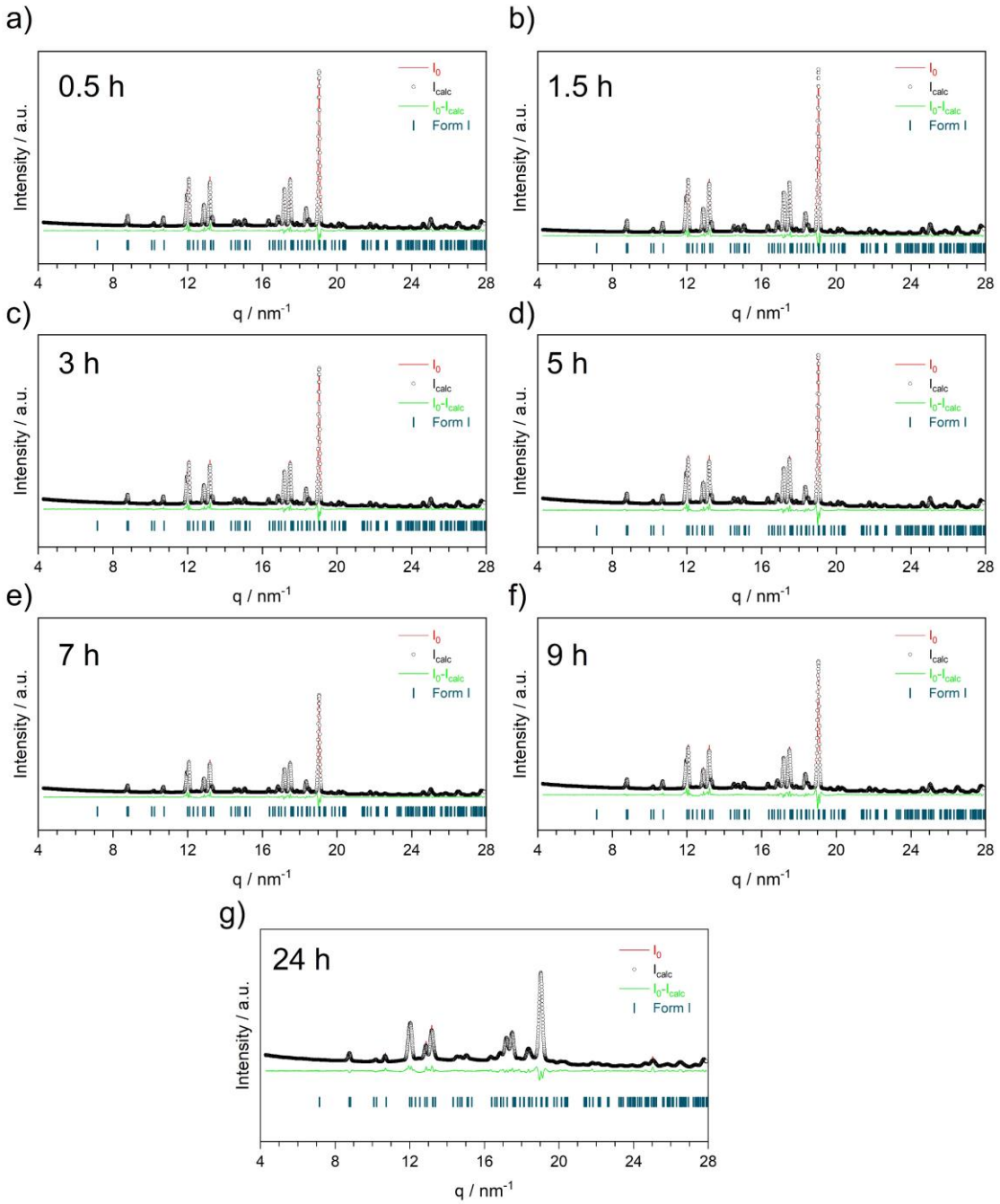

Figure S3.5| Results of the phase analyses for the mechanochemical synthesis of the cocrystal NA:PA with a ball size of 8 mm and a frequency of 35 Hz at ambient temperature: a) at a ball milling time of 0.5 h (R_{wp} = 6.653); b) at a ball milling time of 1.5 h (R_{wp} = 6.649); c) at a ball milling time of 3 h (R_{wp} = 6.354); d) at a ball milling time of 5 h (R_{wp} = 6.158), e) at a ball milling time of 7 h (R_{wp} = 6.633), f) at a ball milling time of 9 h (R_{wp} = 6.961) and g) at a ball milling time of 24 h (R_{wp} = 5.934).

Table S3.5| Results of the Rietveld quantitative phase analyses for the mechanochemical synthesis of the cocrystal NA:PA using an 8 mm milling ball and a frequency of 35 Hz at ambient temperature. The weighted *R*-factor (R_{wp}) is given alongside the crystal sizes (CS) obtained from the Scherrer equation.

time	Reagents /%	Form I / %	Form II / %	R_{wp}	CS (Form I) / nm	CS (Form II) / nm
0.5 h	0	100	0	6.653	167 ± 7	-
1.5 h	0	100	0	6.649	220 ± 16	-
3 h	0	100	0	6.354	178 ± 8	-
5 h	0	100	0	6.158	130 ± 4	-
7 h	0	100	0	6.633	157 ± 7	-
9 h	0	100	0	6.961	144 ± 7	-
24 h	0	100	0	5.934	80 ± 4	-

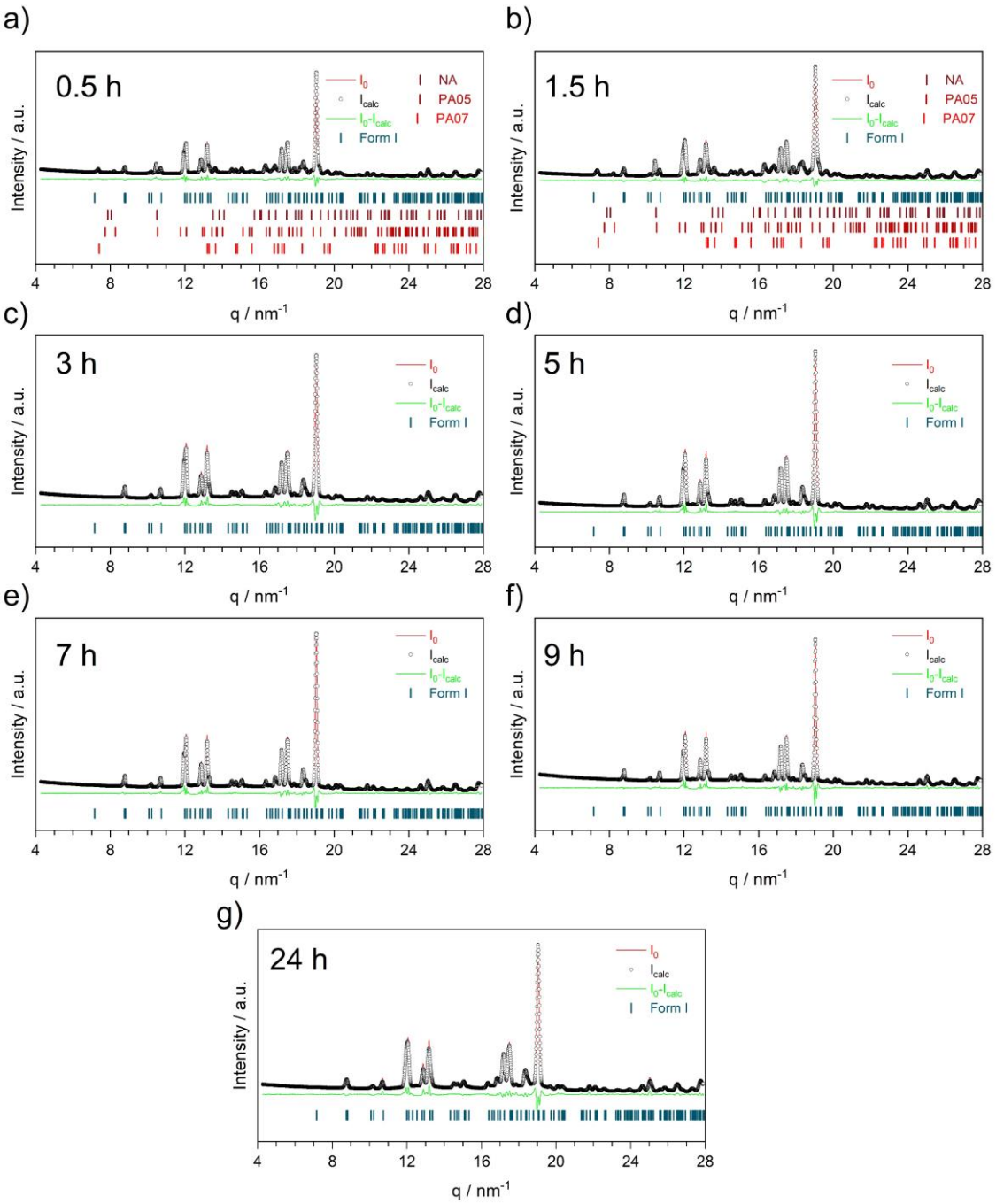

Figure S3.6| Results of the phase analyses for the mechanochemical synthesis of the cocrystal NA:PA with a ball size of 6 mm and a frequency of 35 Hz at ambient temperature: a) at a ball milling time of 0.5 h (R_{wp} = 5.307); b) at a ball milling time of 1.5 h (R_{wp} = 5.410); c) at a ball milling time of 3 h (R_{wp} = 7.107); d) at a ball milling time of 5 h (R_{wp} = 7.631), e) at a ball milling time of 7 h (R_{wp} = 6.707), f) at a ball milling time of 9 h (R_{wp} = 6.995) and g) at a ball milling time of 24 h (R_{wp} = 7.721).

Table S3.6| Results of the Rietveld quantitative phase analyses for the mechanochemical synthesis of the cocrystal NA:PA using a 6 mm milling ball and a frequency of 35 Hz at ambient temperature. The weighted *R*-factor (R_{wp}) is given alongside the crystal sizes (CS) obtained from the Scherrer equation.

time	Reagents /%	Form I / %	Form II / %	R_{wp}	CS (Form I) / nm	CS (Form II) / nm
0.5 h	14	86	0	5.307	83 ± 1	-
1.5 h	18	82	0	5.410	75 ± 1	-
3 h	0	100	0	7.107	120 ± 6	-
5 h	0	100	0	7.631	137 ± 7	-
7 h	0	100	0	6.707	163 ± 9	-
9 h	0	100	0	6.995	192 ± 17	-
24 h	0	100	0	7.721	51 ± 1	-

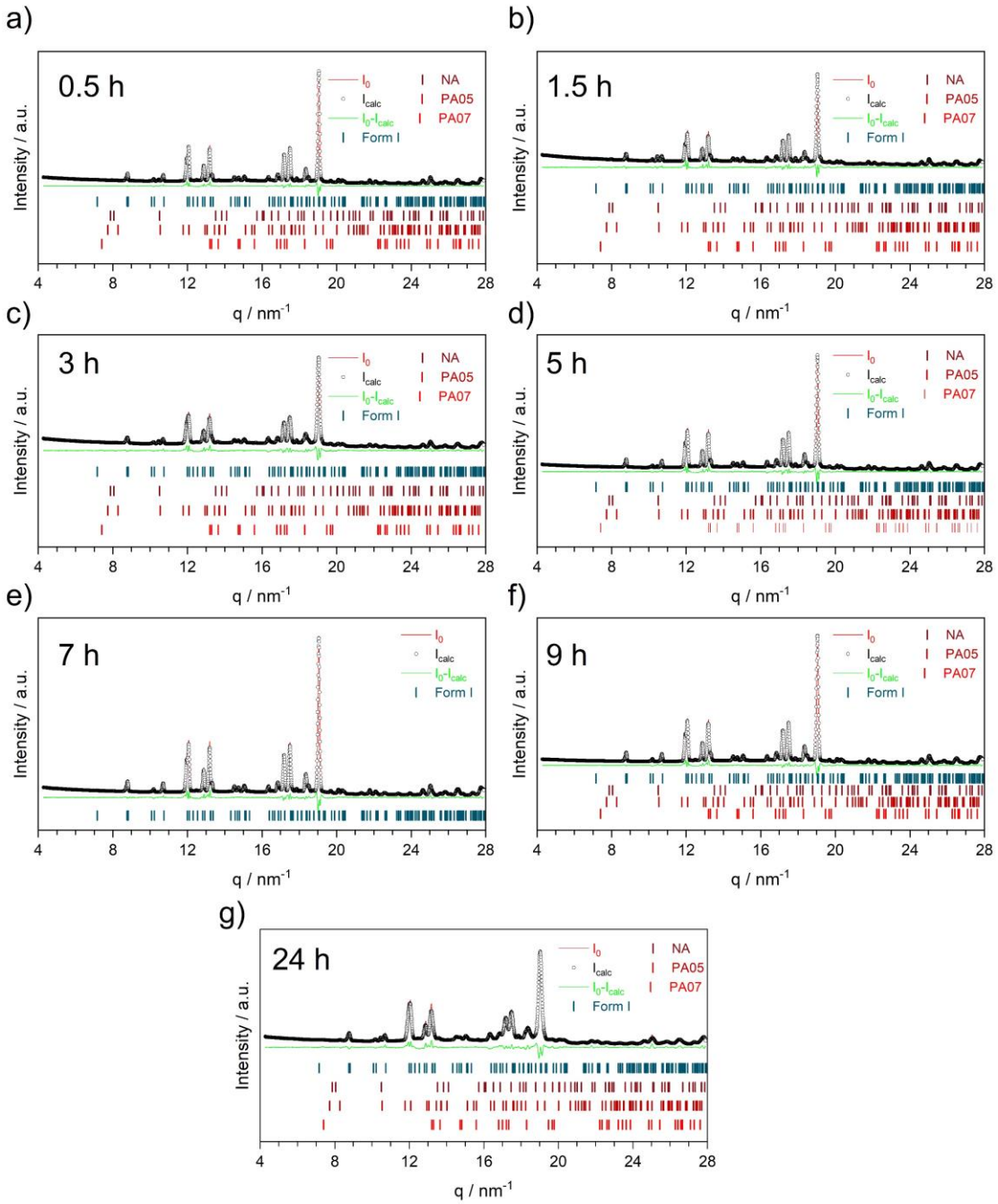

Figure S3.7| Results of the phase analyses for the mechanochemical synthesis of the cocrystal NA:PA with a ball size of 10 mm and a frequency of 20 Hz at ambient temperature: a) at a ball milling time of 0.5 h (R_{wp} = 5.490); b) at a ball milling time of 1.5 h (R_{wp} = 6.509); c) at a ball milling time of 3 h (R_{wp} = 6.217); d) at a ball milling time of 5 h (R_{wp} = 7.014), e) at a ball milling time of 7 h (R_{wp} = 6.903), f) at a ball milling time of 9 h (R_{wp} = 6.686) and g) at a ball milling time of 24 h (R_{wp} = 7.436).

Table S3.7| Results of the Rietveld quantitative phase analyses for the mechanochemical synthesis of the cocrystal NA:PA using a 10 mm milling ball and a frequency of 20 Hz at ambient temperature. The weighted *R*-factor (R_{wp}) is given alongside the crystal sizes (CS) obtained from the Scherrer equation.

time	Reagents /%	Form I / %	Form II / %	R_{wp}	CS (Form I) / nm	CS (Form II) / nm
0.5 h	3	97	0	5.490	249 ± 19	-
1.5 h	7	93	0	6.509	69 ± 1	-
3 h	5	95	0	6.217	77 ± 2	-
5 h	2	98	0	7.014	187 ± 13	-
7 h	0	100	0	6.903	149 ± 6	-
9 h	1	99	0	6.686	170 ± 10	-
24 h	5	95	0	7.436	83 ± 4	-

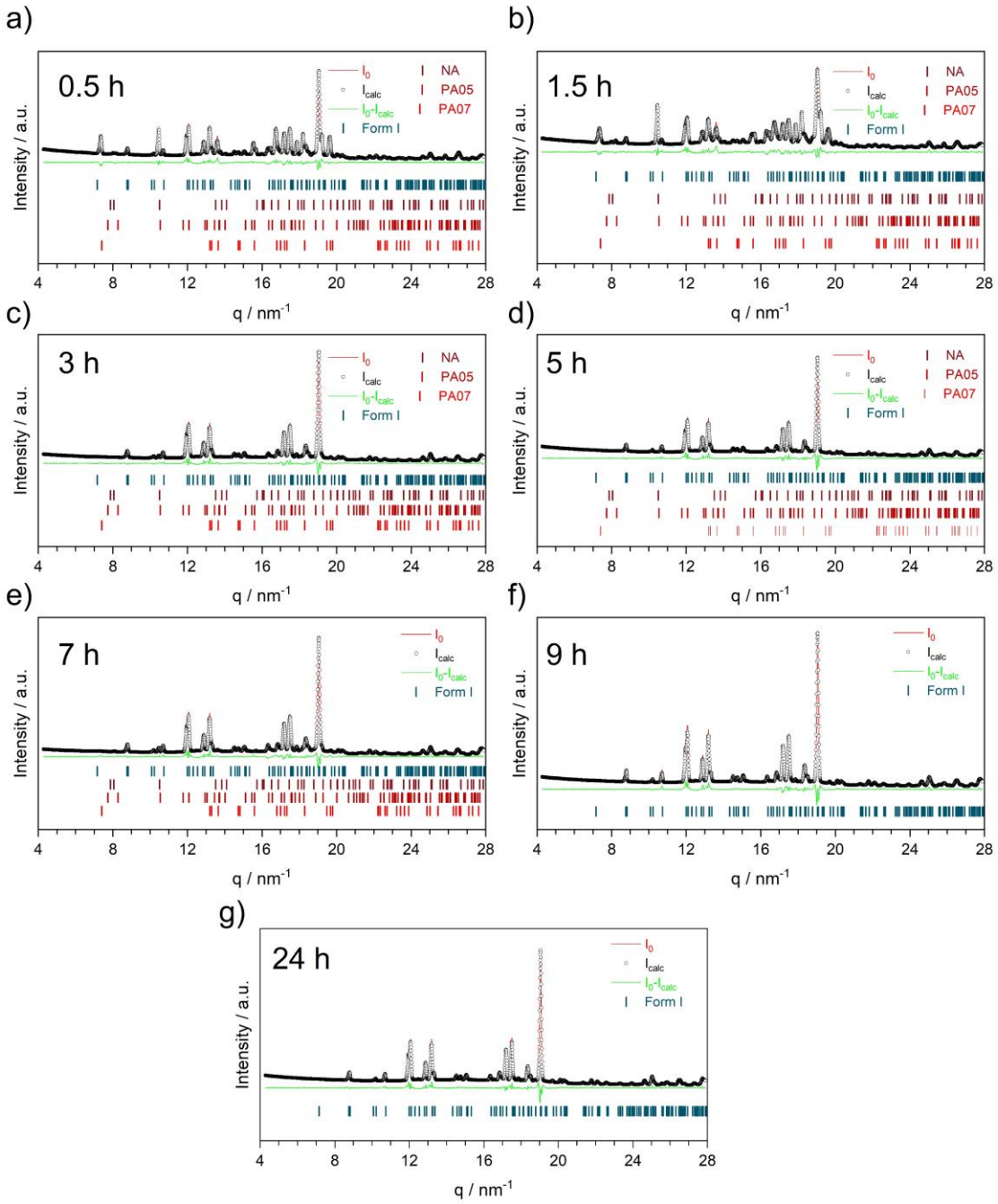

Figure S3.8| Results of the phase analyses for the mechanochemical synthesis of the cocrystal NA:PA with a ball size of 8 mm and a frequency of 20 Hz at ambient temperature: a) at a ball milling time of 0.5 h (R_{wp} = 5.618); b) at a ball milling time of 1.5 h (R_{wp} = 5.711); c) at a ball milling time of 3 h (R_{wp} = 6.608); d) at a ball milling time of 5 h (R_{wp} = 7.039), e) at a ball milling time of 7 h (R_{wp} = 7.333), f) at a ball milling time of 9 h (R_{wp} = 6.703) and g) at a ball milling time of 24 h (R_{wp} = 5.958).

Table S3.8| Results of the Rietveld quantitative phase analyses for the mechanochemical synthesis of the cocrystal NA:PA using an 8 mm milling ball and a frequency of 20 Hz at ambient temperature. The weighted *R*-factor (R_{wp}) is given alongside the crystal sizes (CS) obtained from the Scherrer equation.

time	Reagents /%	Form I / %	Form II / %	R_{wp}	CS (Form I) / nm	CS (Form II) / nm
0.5 h	32	68	0	5.618	215 ± 30	-
1.5 h	40	60	0	5.711	102 ± 6	-
3 h	2	98	0	6.608	86 ± 2	-
5 h	1	99	0	7.039	148 ± 11	-
7 h	3	97	0	7.333	117 ± 4	-
9 h	0	100	0	6.703	-	-
24 h	0	100	0	5.958	125 ± 3	-

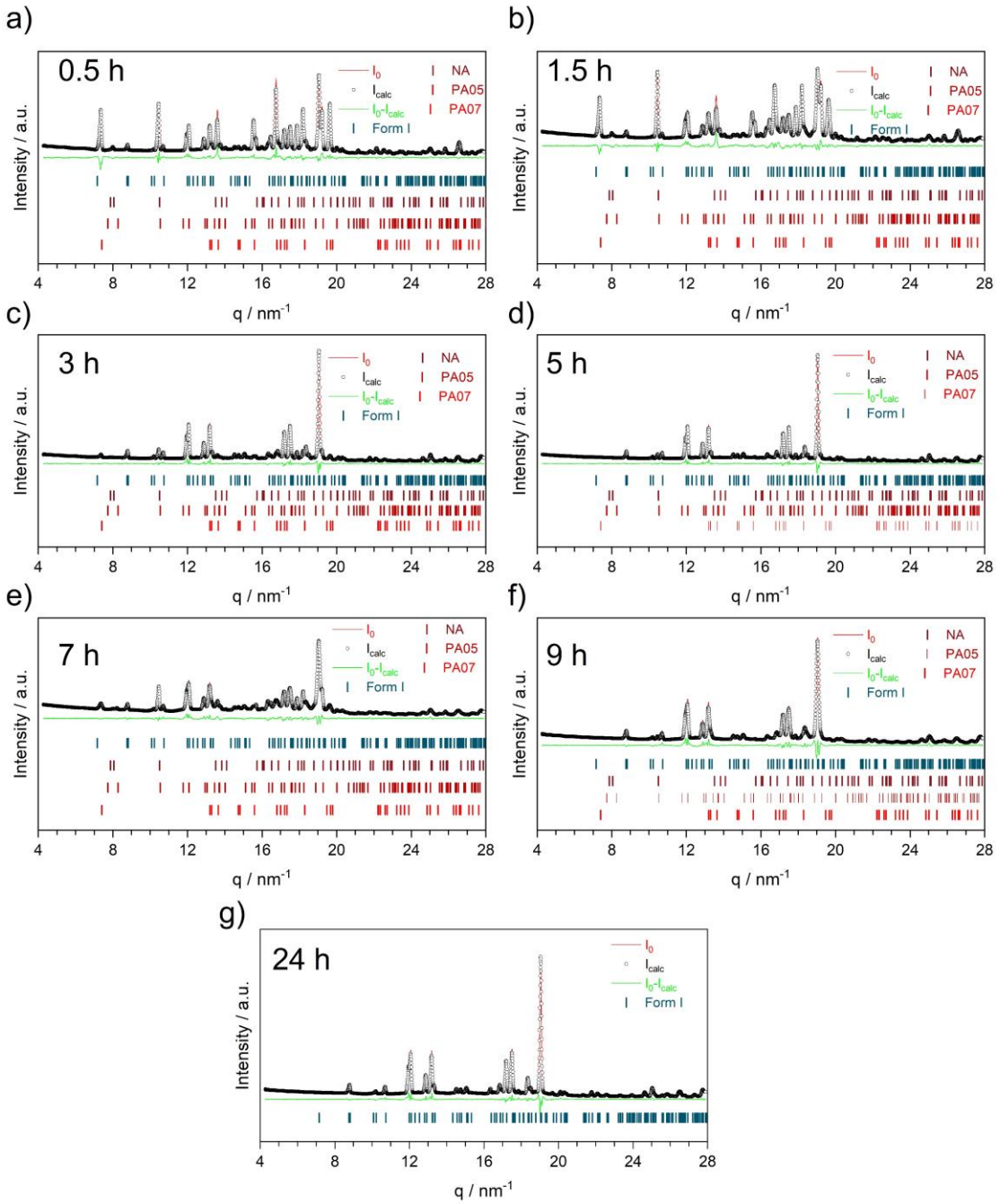

Figure S3.9| Results of the phase analyses for the mechanochemical synthesis of the cocrystal NA:PA with a ball size of 6 mm and a frequency of 20 Hz at ambient temperature: a) at a ball milling time of 0.5 h (R_{wp} = 7.157); b) at a ball milling time of 1.5 h (R_{wp} = 6.623); c) at a ball milling time of 3 h (R_{wp} = 5.374); d) at a ball milling time of 5 h (R_{wp} = 5.371), e) at a ball milling time of 7 h (R_{wp} = 4.786), f) at a ball milling time of 9 h (R_{wp} = 7.537) and g) at a ball milling time of 24 h (R_{wp} = 6.520).

Table S3.9| Results of the Rietveld quantitative phase analyses for the mechanochemical synthesis of the cocrystal NA:PA using a 6 mm milling ball and a frequency of 20 Hz at ambient temperature. The weighted *R*-factor (R_{wp}) is given alongside the crystal sizes (CS) obtained from the Scherrer equation.

time	Reagents /%	Form I / %	Form II / %	R_{wp}	CS (Form I) / nm	CS (Form II) / nm
0.5 h	54	46	0	7.157	-	-
1.5 h	54	46	0	6.623	211. ± 57	-
3 h	12	88	0	5.374	230 ± 17	-
5 h	4	96	0	5.371	219 ± 15	-
7 h	28	72	0	4.786	-	-
9 h	3	97	0	7.537	143 ± 14	-
24 h	0	100	0	6.520	117 ± 3	-

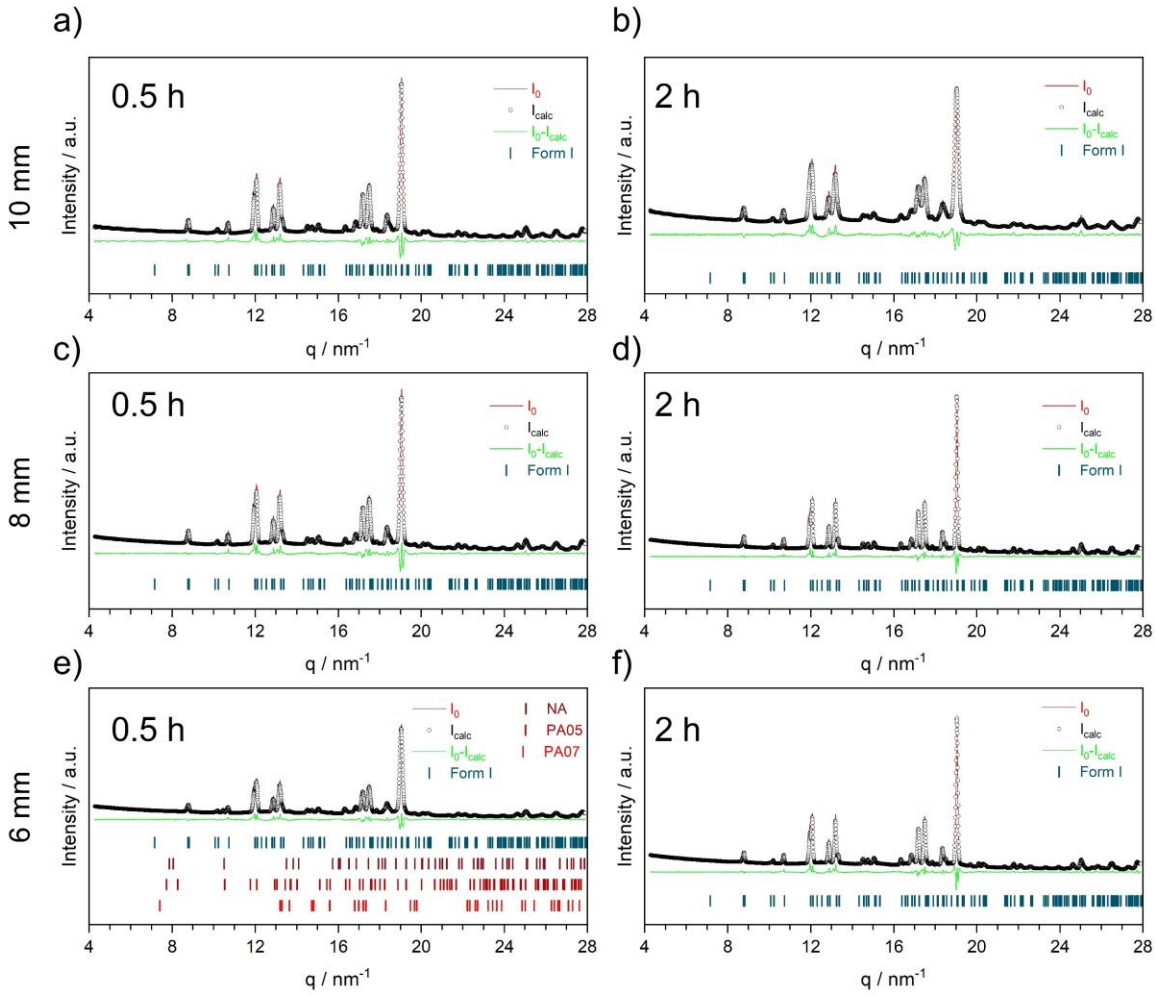

Figure S3.10| Results of the phase analyses for the mechanochemical synthesis of the cocrystal NA:PA with three different ball size (10, 8 and 6 mm) and a frequency of 50 Hz at 55°C: ball milling with a ball size of 10 mm (a: ball milling time of 0.5 h (R_{wp} = 6.835) and b: ball milling time of 2 h (R_{wp} = 6.123)); ball milling with a ball size of 8 mm (c: ball milling time of 0.5 h (R_{wp} = 7.038) and d: ball milling time of 2 h (R_{wp} = 7.087); ball milling with a ball size of 6 mm(e: ball milling time of 0.5 h (R_{wp} = 6.460) and f: ball milling time of 2 h (R_{wp} = 6.581).

Table S3.10| Results of the Rietveld quantitative phase analyses for the mechanochemical synthesis of the cocrystal NA:PA using three different ball sizes (10, 8 and 6 mm) and at a frequency of 50 Hz at 55°C.

Ball size	*time*	Reagents /%	Form I / %	Form II / %	R_{wp}
10	0.5 h	0	100	0	6.835
	2 h	0	100	0	5.970
8	0.5 h	0	100	0	7.038
	2 h	0	100	0	7.087
6	0.5 h	4	96	0	6.460
	2 h	0	100	0	6.581

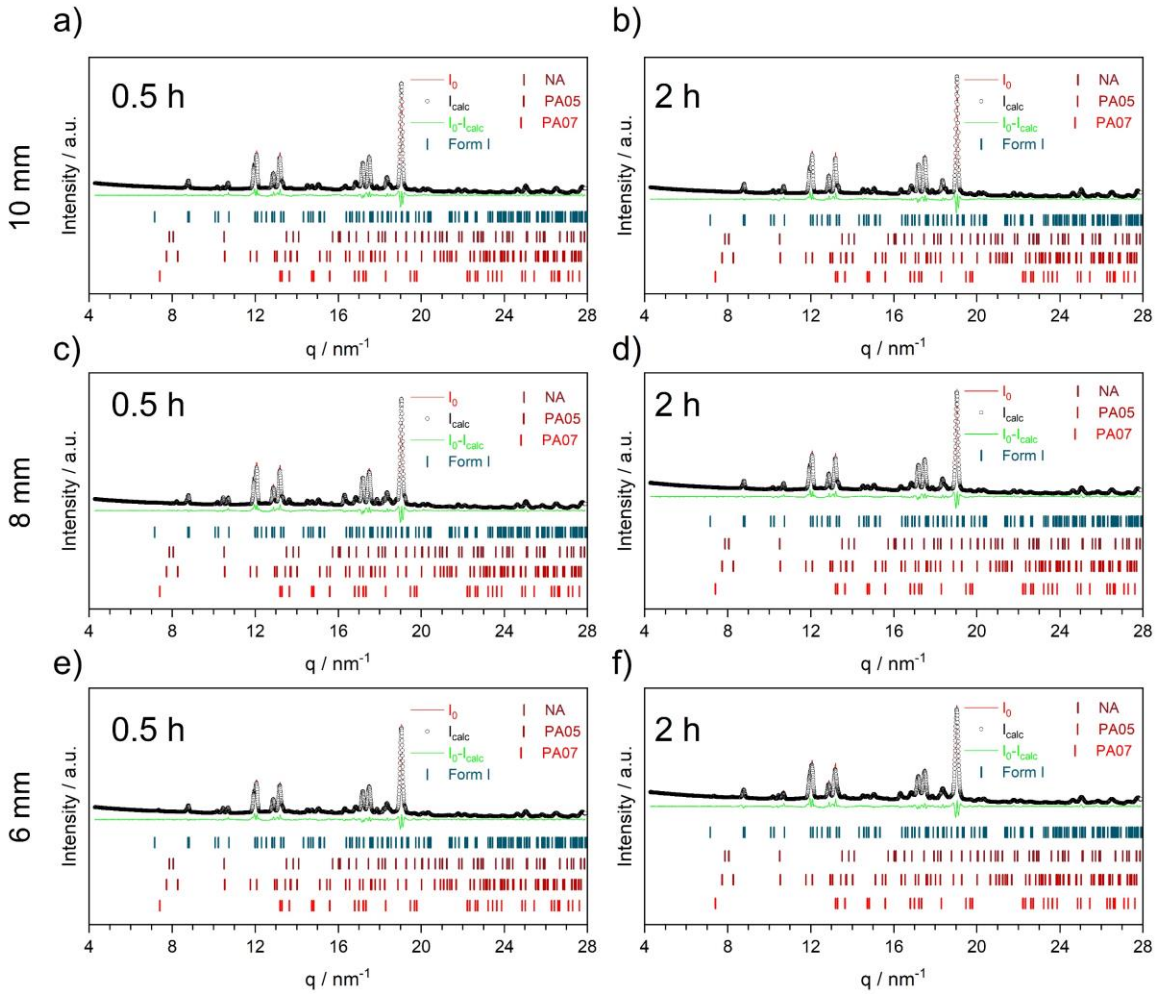

Figure S3.11| Results of the phase analyses for the mechanochemical synthesis of the cocrystal NA:PA with three different ball size (10, 8 and 6 mm) and a frequency of 35 Hz at 55°C: ball milling with a ball size of 10 mm (a: ball milling time of 0.5 h (R_{wp} = 6.865) and b: ball milling time of 2 h (R_{wp} = 7.272)); ball milling with a ball size of 8 mm (c: ball milling time of 0.5 h (R_{wp} = 6.832) and d: ball milling time of 2 h (R_{wp} = 6.550); ball milling with a ball size of 6 mm(e: ball milling time of 0.5 h (R_{wp} = 6.040) and f: ball milling time of 2 h (R_{wp} = 6.596).

Table S3.11| Results of the Rietveld quantitative phase analyses for the mechanochemical synthesis of the cocrystal NA:PA using three different ball sizes (10, 8 and 6 mm) and at a frequency of 35 Hz at 55°C.

Ball size	*time*	Reagents /%	Form I / %	Form II / %	R_{wp}
10	0.5 h	3	97	0	6.865
	2 h	2	98	0	7.272
8	0.5 h	10	90	0	6.832
	2 h	2	98	0	6.550
6	0.5 h	7	93	0	6.040
	2 h	5	95	0	6.596

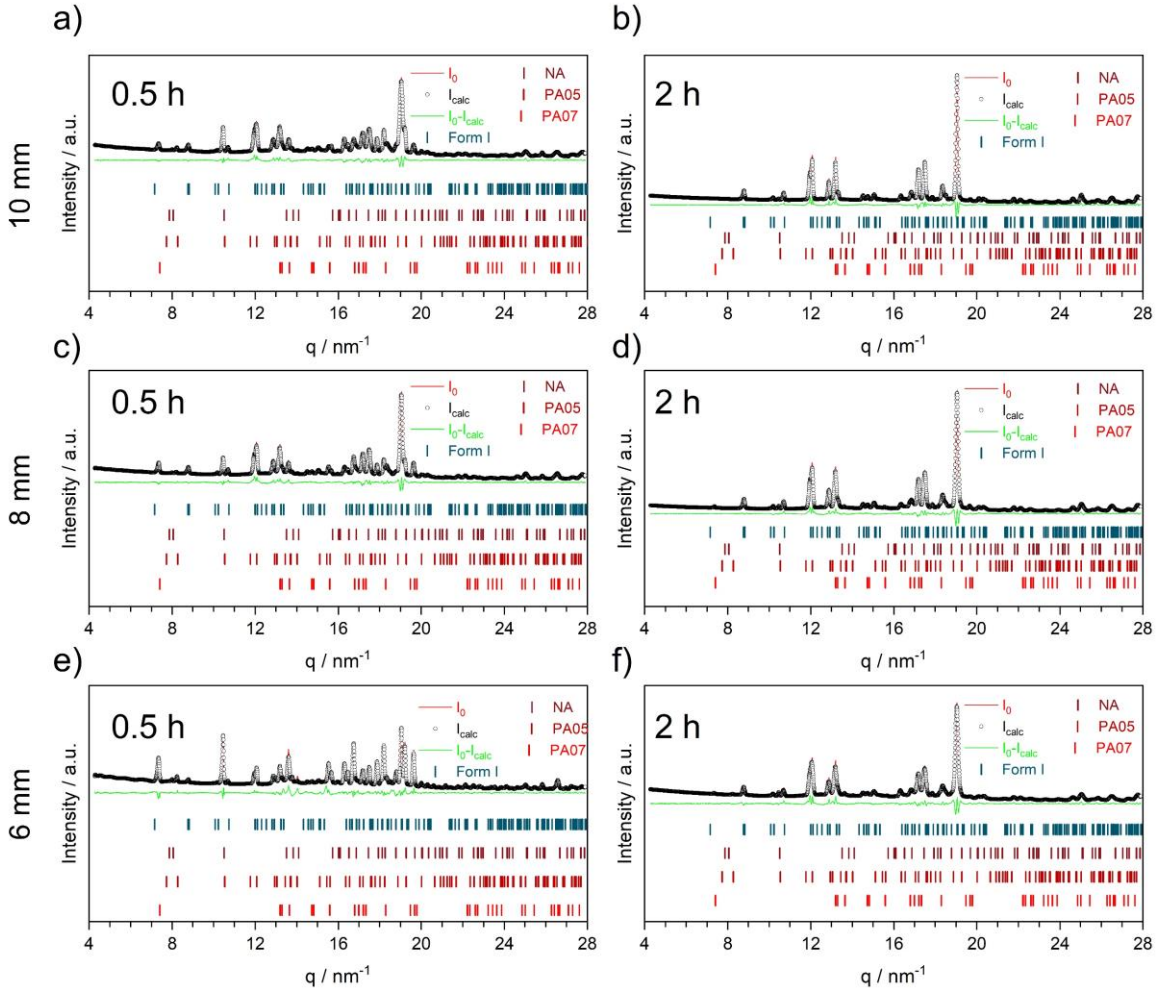

Figure S3.12| Results of the phase analyses for the mechanochemical synthesis of the cocrystal NA:PA with three different ball size (10, 8 and 6 mm) and a frequency of 20 Hz at 55°C: ball milling with a ball size of 10 mm (a: ball milling time of 0.5 h (R_{wp} = 5.035) and b: ball milling time of 2 h (R_{wp} = 7.317)); ball milling with a ball size of 8 mm (c: ball milling time of 0.5 h (R_{wp} = 5.735) and d: ball milling time of 2 h (R_{wp} = 7.236); ball milling with a ball size of 6 mm(e: ball milling time of 0.5 h (R_{wp} =) and f: ball milling time of 2 h (R_{wp} = 5.945).

Table S3.12| Results of the Rietveld quantitative phase analyses for the mechanochemical synthesis of the cocrystal NA:PA using three different ball sizes (10, 8 and 6 mm) and at a frequency of 20 Hz at 55°C.

Ball size	***time***	**Reagents /%**	**Form I / %**	**Form II / %**	**R_{wp}**
10	0.5 h	28	72	0	5.035
	2 h	1	99	0	7.317
8	0.5 h	24	76	0	5.735
	2 h	3	97	0	7.236
6	0.5 h	64	36	0	7.121
	2 h	14	86	0	5.945

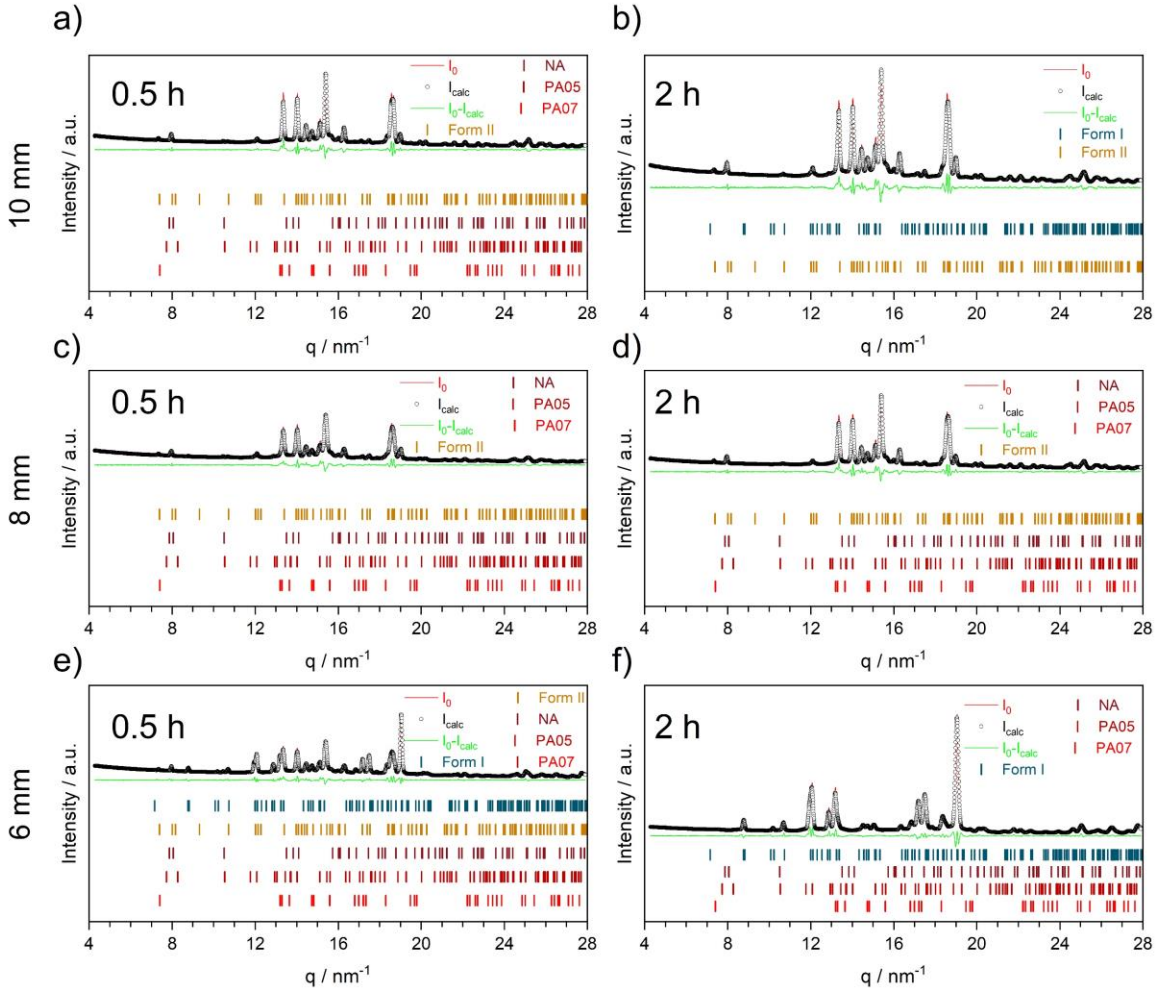

Figure S3.13| Results of the phase analyses for the mechanochemical synthesis of the cocrystal NA:PA with three different ball size (10, 8 and 6 mm) and a frequency of 50 Hz at 65°C: ball milling with a ball size of 10 mm (a: ball milling time of 0.5 h (R_{wp} = 6.509) and b: ball milling time of 2 h (R_{wp} = 6.336)); ball milling with a ball size of 8 mm (c: ball milling time of 0.5 h (R_{wp} = 5.451) and d: ball milling time of 2 h (R_{wp} = 6.640); ball milling with a ball size of 6 mm(e: ball milling time of 0.5 h (R_{wp} = 4.882) and f: ball milling time of 2 h (R_{wp} = 7.044).

Table S3.13| Results of the Rietveld quantitative phase analyses for the mechanochemical synthesis of the cocrystal NA:PA using three different ball sizes (10, 8 and 6 mm) and at a frequency of 50 Hz at 65°C.

Ball size	***time***	**Reagents /%**	**Form I / %**	**Form II / %**	**R_{wp}**
10	0.5 h	1	0	99	6.509
	2 h	0	2	98	6.336
8	0.5 h	7	0	93	5.451
	2 h	0	0	100	6.640
6	0.5 h	1	48	51	4.882
	2 h	0	100	0	7.044

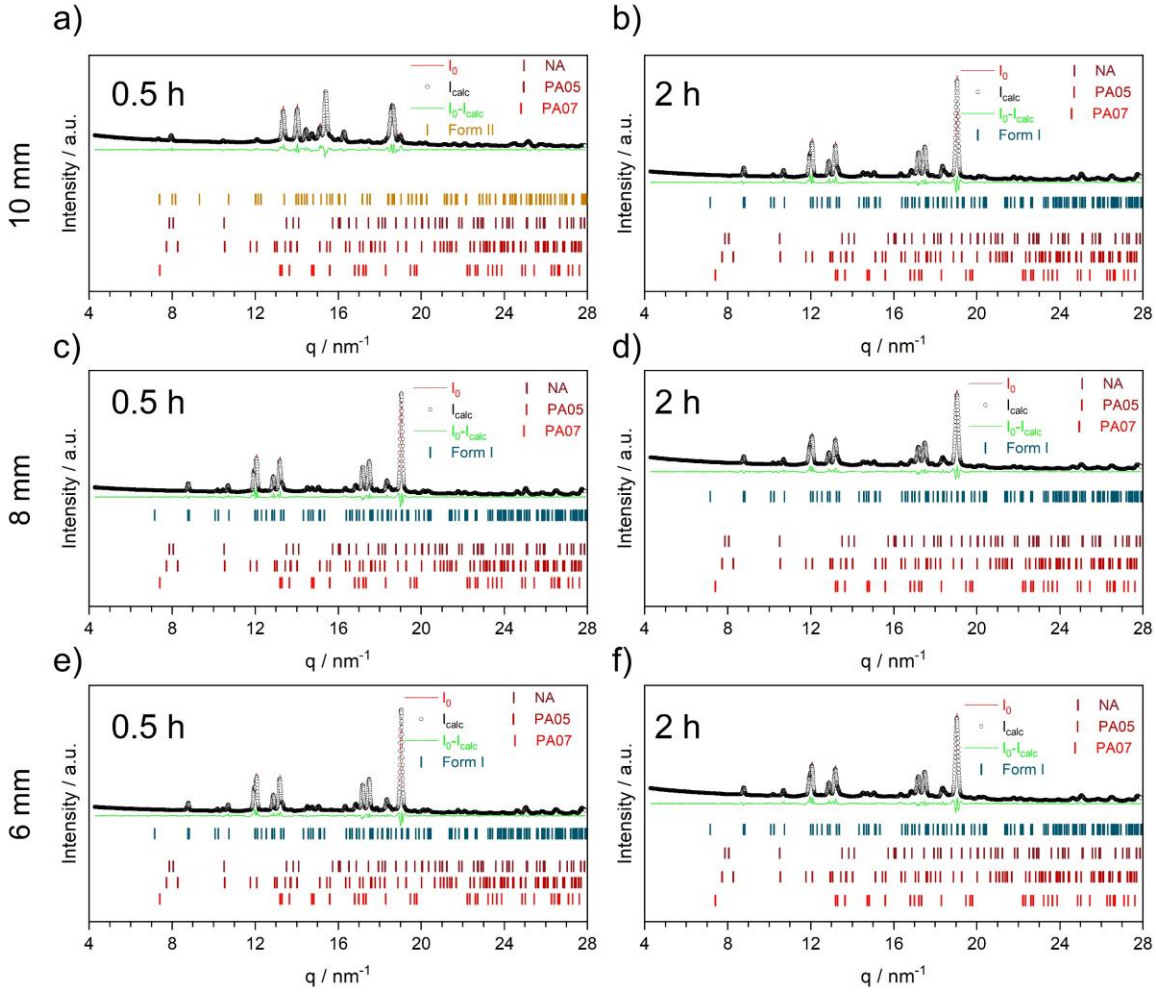

Figure S3.14| Results of the phase analyses for the mechanochemical synthesis of the cocrystal NA:PA with three different ball size (10, 8 and 6 mm) and a frequency of 35 Hz at 65°C: ball milling with a ball size of 10 mm (a: ball milling time of 0.5 h (R_{wp} = 6.363) and b: ball milling time of 2 h (R_{wp} = 6.801)); ball milling with a ball size of 8 mm (c: ball milling time of 0.5 h (R_{wp} = 6.625) and d: ball milling time of 2 h (R_{wp} = 5.626); ball milling with a ball size of 6 mm(e: ball milling time of 0.5 h (R_{wp} = 6.163) and f: ball milling time of 2 h (R_{wp} = 5.941).

Table S3.14| Results of the Rietveld quantitative phase analyses for the mechanochemical synthesis of the cocrystal NA:PA using three different ball sizes (10, 8 and 6 mm) and at a frequency of 35 Hz at 65°C.

Ball size	***time***	**Reagents /%**	**Form I / %**	**Form II / %**	**R_{wp}**
10	0.5 h	2	0	98	6.363
	2 h	0	100	0	6.801
8	0.5 h	2	98	0	6.625
	2 h	2	98	0	5.626
6	0.5 h	2	98	0	6.163
	2 h	0	100	0	5.941

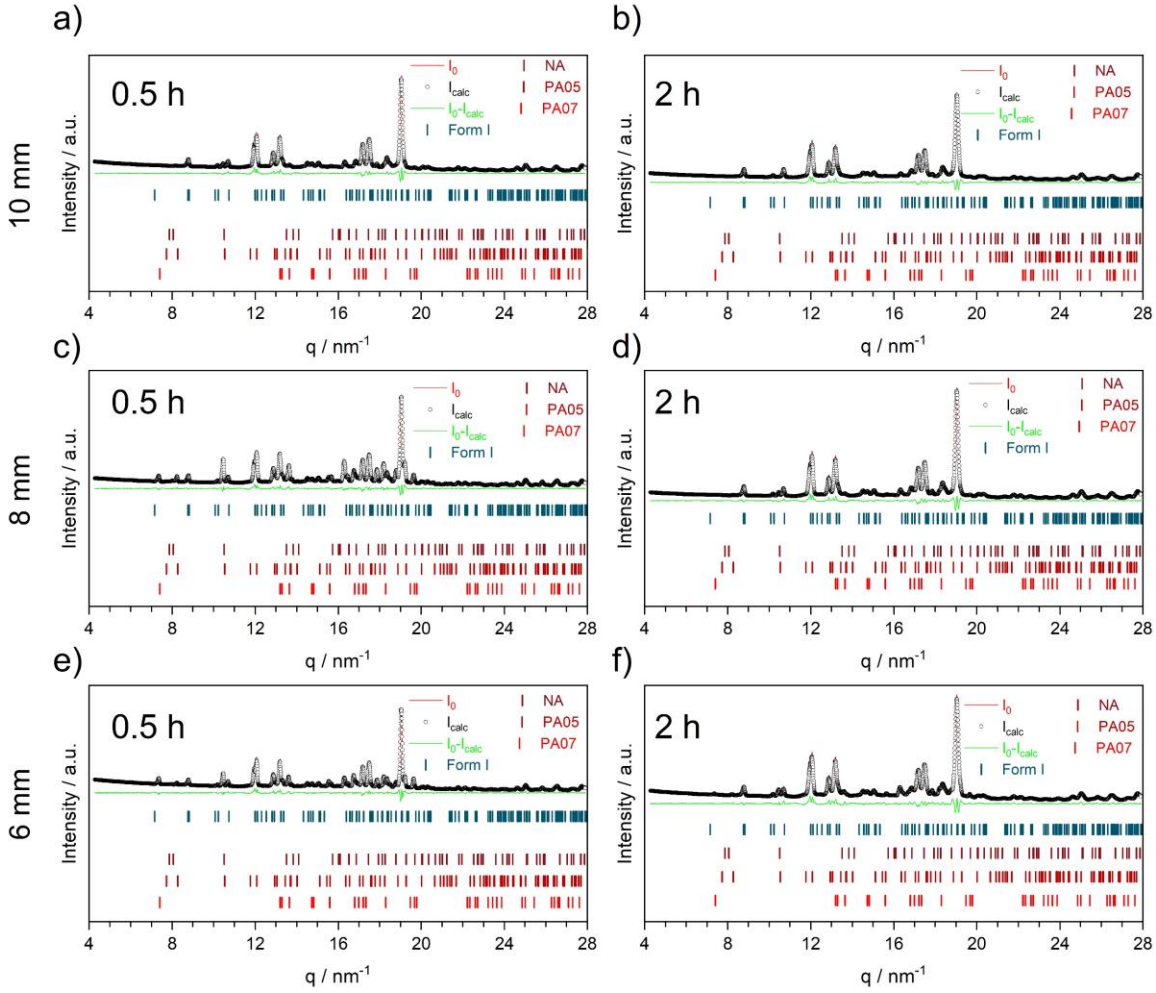

Figure S3.15| Results of the phase analyses for the mechanochemical synthesis of the cocrystal NA:PA with three different ball size (10, 8 and 6 mm) and a frequency of 20 Hz at 65°C: ball milling with a ball size of 10 mm (a: ball milling time of 0.5 h (R_{wp} = 5.536) and b: ball milling time of 2 h (R_{wp} = 6.108)); ball milling with a ball size of 8 mm (c: ball milling time of 0.5 h (R_{wp} = 4.919) and d: ball milling time of 2 h (R_{wp} = 6.529); ball milling with a ball size of 6 mm(e: ball milling time of 0.5 h (R_{wp} =) and f: ball milling time of 2 h (R_{wp} = 6.229).

Table S3.15| Results of the Rietveld quantitative phase analyses for the mechanochemical synthesis of the cocrystal NA:PA using three different ball sizes (10, 8 and 6 mm) and at a frequency of 20 Hz at 65°C.

Ball size	***time***	**Reagents /%**	**Form I / %**	**Form II / %**	**R_{wp}**
10	0.5 h	6	94	0	5.536
	2 h	1	99	0	6.108
8	0.5 h	32	68	0	4.919
	2 h	4	96	0	6.529
6	0.5 h	24	76	0	4.952
	2 h	9	91	0	6.229

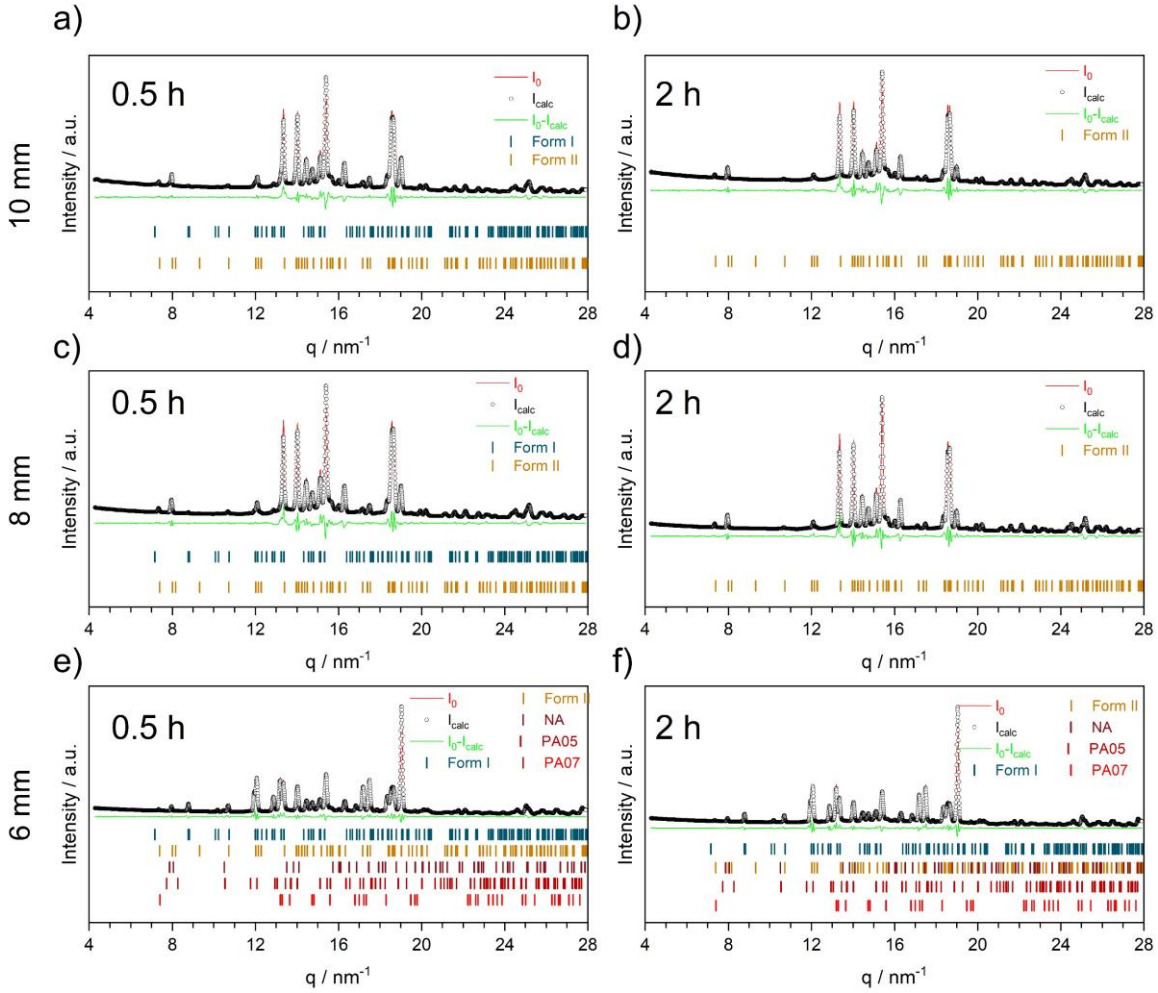

Figure S3.16| Results of the phase analyses for the mechanochemical synthesis of the cocrystal NA:PA with three different ball size (10, 8 and 6 mm) and a frequency of 50 Hz at 75°C: ball milling with a ball size of 10 mm (a: ball milling time of 0.5 h (R_{wp} = 6.012) and b: ball milling time of 2 h (R_{wp} = 7.009)); ball milling with a ball size of 8 mm (c: ball milling time of 0.5 h (R_{wp} = 7.161) and d: ball milling time of 2 h (R_{wp} = 8.189); ball milling with a ball size of 6 mm(e: ball milling time of 0.5 h (R_{wp} = 5.917) and f: ball milling time of 2 h (R_{wp} = 6.053).

Table S3.16| Results of the Rietveld quantitative phase analyses for the mechanochemical synthesis of the cocrystal NA:PA using three different ball sizes (10, 8 and 6 mm) and at a frequency of 50 Hz at 75°C.

Ball size	***time***	**Reagents /%**	**Form I / %**	**Form II / %**	**R_{wp}**
10	0.5 h	0	94	6	6.012
	2 h	0	0	100	7.009
8	0.5 h	0	4	96	7.161
	2 h	0	0	100	8.189
6	0.5 h	2	61	37	5.917
	2 h	0	68	32	6.053

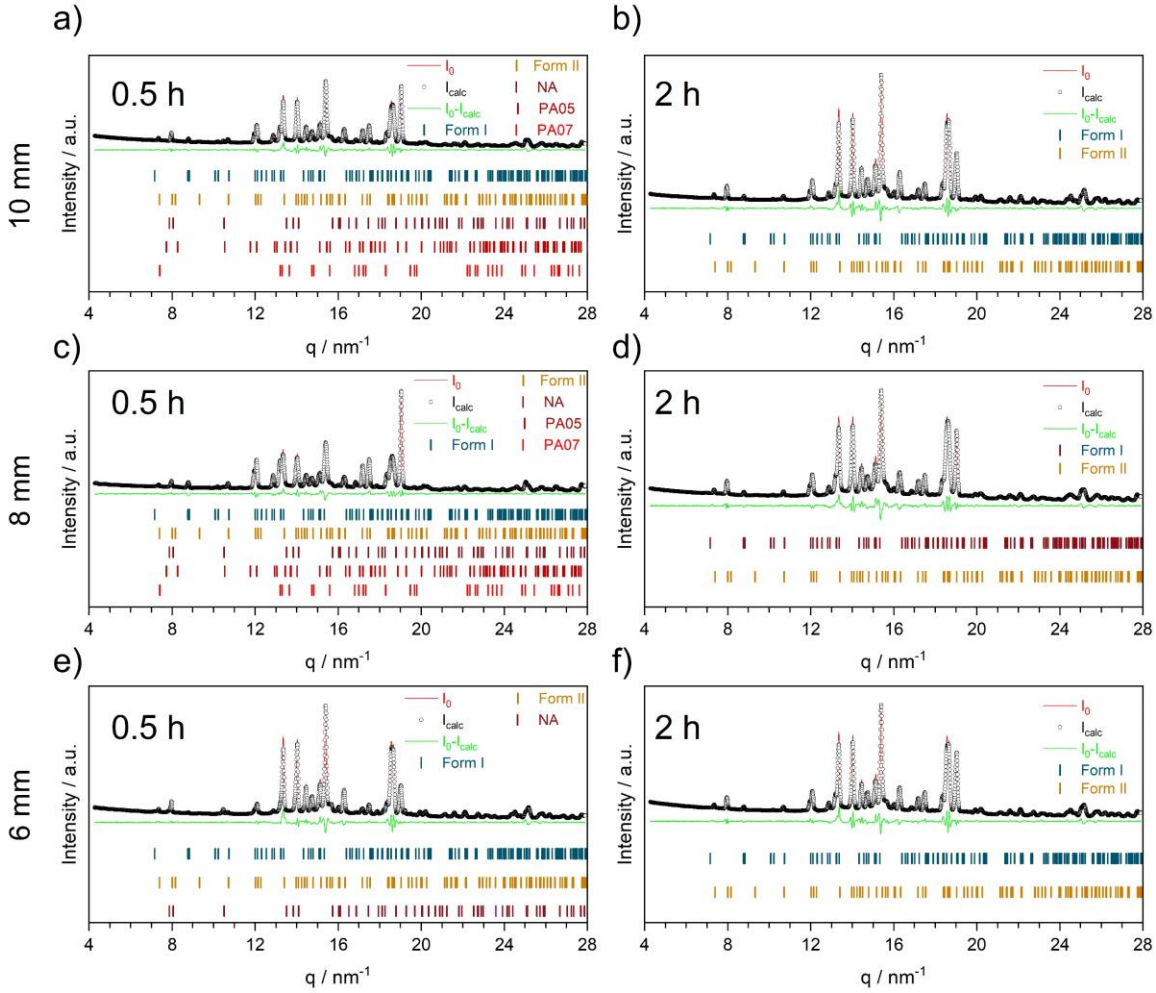

Figure S3.17| Results of the phase analyses for the mechanochemical synthesis of the cocrystal NA:PA with three different ball size (10, 8 and 6 mm) and a frequency of 35 Hz at 75°C: ball milling with a ball size of 10 mm (a: ball milling time of 0.5 h (R_{wp} = 5.893) and b: ball milling time of 2 h (R_{wp} = 7.066)); ball milling with a ball size of 8 mm (c: ball milling time of 0.5 h (R_{wp} = 5.712) and d: ball milling time of 2 h (R_{wp} = 6.481); ball milling with a ball size of 6 mm(e: ball milling time of 0.5 h (R_{wp} = 6.261) and f: ball milling time of 2 h (R_{wp} = 6.469).

Table S3.17| Results of the Rietveld quantitative phase analyses for the mechanochemical synthesis of the cocrystal NA:PA using three different ball sizes (10, 8 and 6 mm) and at a frequency of 35 Hz at 75°C.

Ball size	***time***	**Reagents /%**	**Form I / %**	**Form II / %**	**R_{wp}**
10	0.5 h	1	32	67	5.893
	2 h	0	16	84	7.066
8	0.5 h	1	50	49	5.712
	2 h	0	21	79	6.481
6	0.5 h	3	88	9	6.261
	2 h	0	21	77	6.469

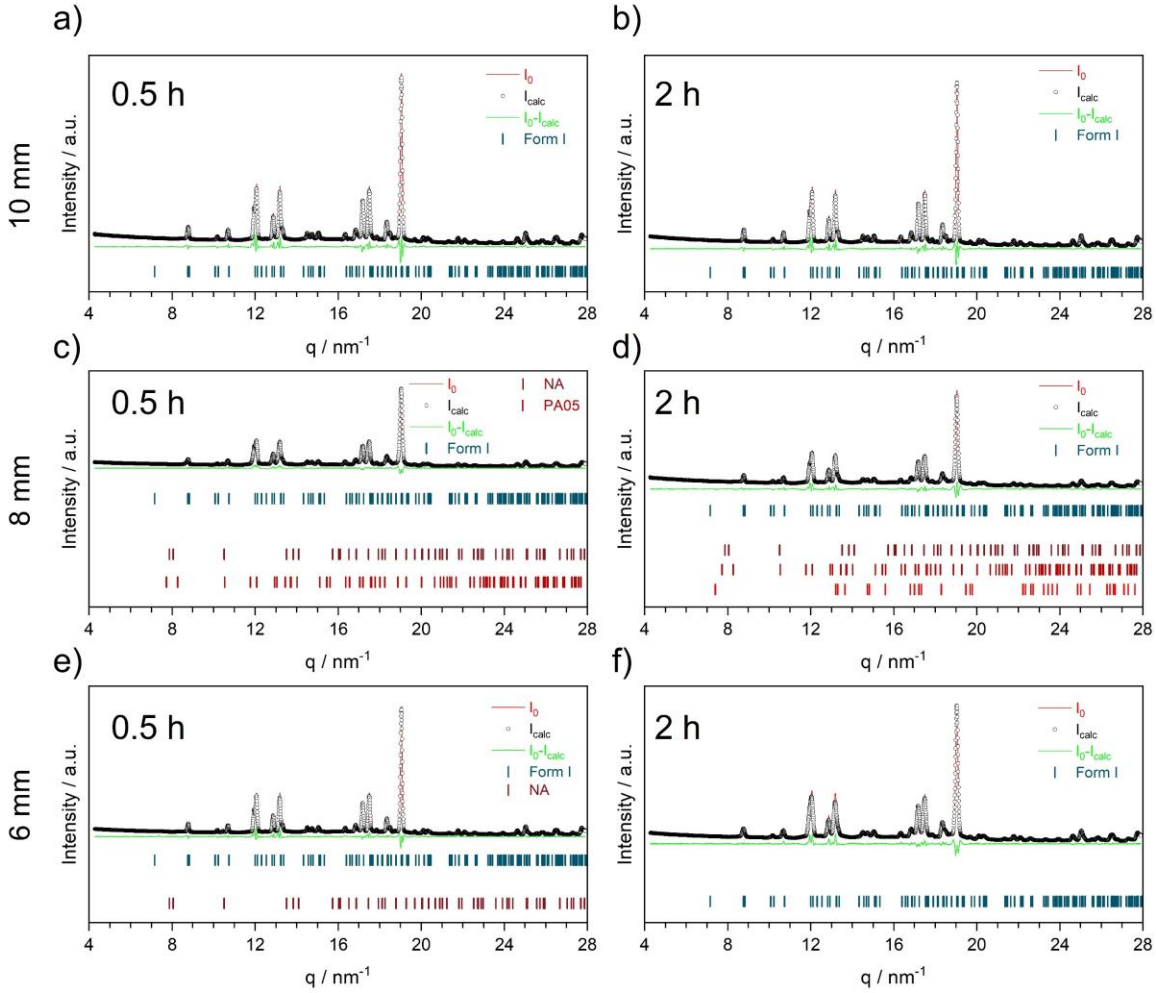

Figure S3.18| Results of the phase analyses for the mechanochemical synthesis of the cocrystal NA:PA with three different ball size (10, 8 and 6 mm) and a frequency of 20 Hz at 75°C: ball milling with a ball size of 10 mm (a: ball milling time of 0.5 h (R_{wp} = 6.991) and b: ball milling time of 2 h (R_{wp} = 7.127)); ball milling with a ball size of 8 mm (c: ball milling time of 0.5 h (R_{wp} = 6.003) and d: ball milling time of 2 h (R_{wp} = 6.268); ball milling with a ball size of 6 mm(e: ball milling time of 0.5 h (R_{wp} = 6.387) and f: ball milling time of 2 h (R_{wp} = 6.896).

Table S3.18| Results of the Rietveld quantitative phase analyses for the mechanochemical synthesis of the cocrystal NA:PA using three different ball sizes (10, 8 and 6 mm) and at a frequency of 20 Hz at 75°C.

Ball size	***time***	**Reagents /%**	**Form I / %**	**Form II / %**	**R_{wp}**
10	0.5 h	0	100	0	6.991
	2 h	0	100	0	7.127
8	0.5 h	2	98	0	6.003
	2 h	2	98	0	6.268
6	0.5 h	1	99	0	6.387
	2 h	0	100	0	6.896

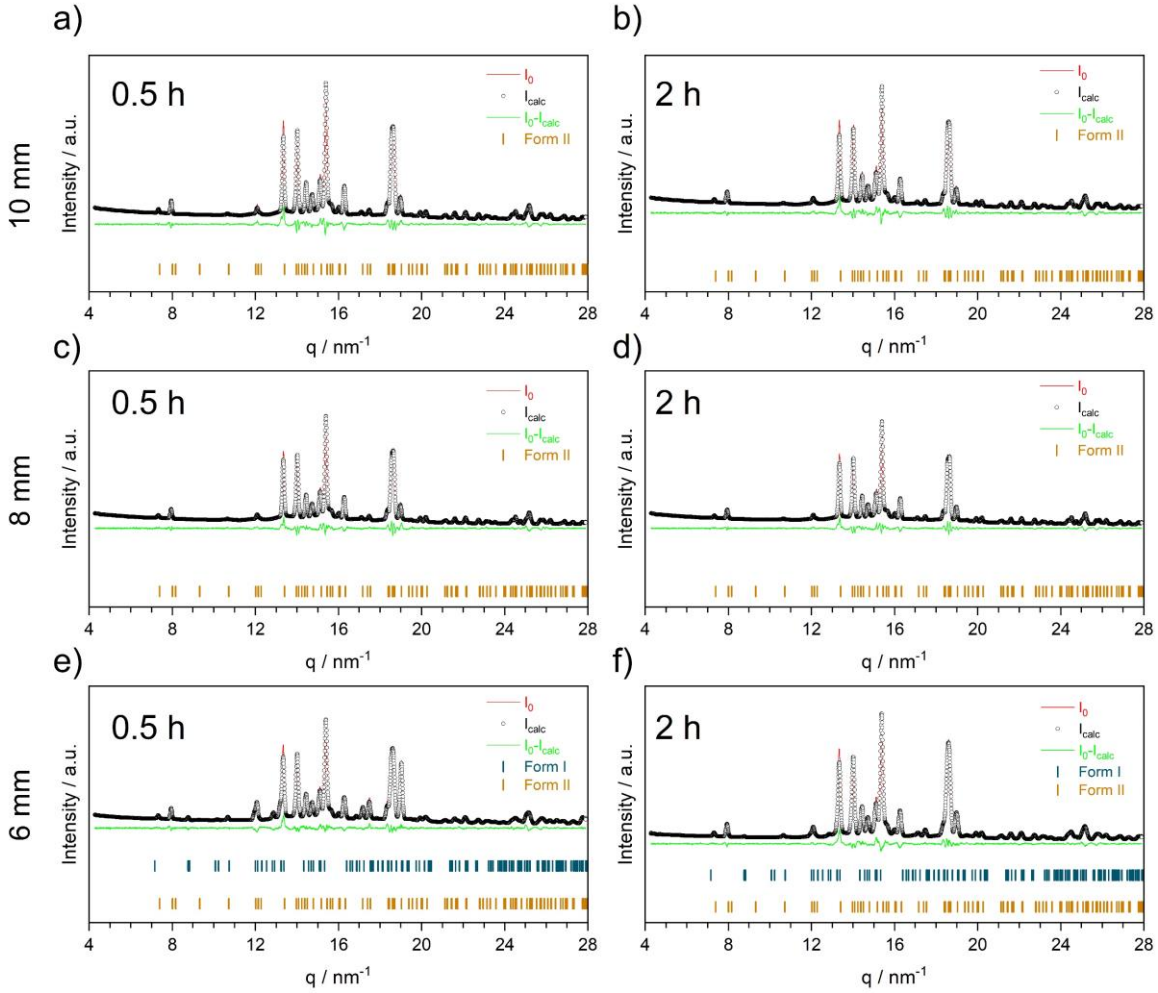

Figure S3.19| Results of the phase analyses for the mechanochemical synthesis of the cocrystal NA:PA with three different ball size (10, 8 and 6 mm) and a frequency of 50 Hz at 80°C: ball milling with a ball size of 10 mm (a: ball milling time of 0.5 h (R_{wp} = 7.053) and b: ball milling time of 2 h (R_{wp} = 7.193)); ball milling with a ball size of 8 mm (c: ball milling time of 0.5 h (R_{wp} = 6.860) and d: ball milling time of 2 h (R_{wp} = 6.149); ball milling with a ball size of 6 mm(e: ball milling time of 0.5 h (R_{wp} = 6.617) and f: ball milling time of 2 h (R_{wp} = 6.723).

Table S3.19| Results of the Rietveld quantitative phase analyses for the mechanochemical synthesis of the cocrystal NA:PA using three different ball sizes (10, 8 and 6 mm) and at a frequency of 50 Hz at 80°C.

Ball size	***time***	**Reagents /%**	**Form I / %**	**Form II / %**	**R_{wp}**
10	0.5 h	0	0	100	7.053
	2 h	0	0	100	7.193
8	0.5 h	0	0	100	6.860
	2 h	0	0	100	6.149
6	0.5 h	0	22	78	6.617
	2 h	0	6	94	6.723

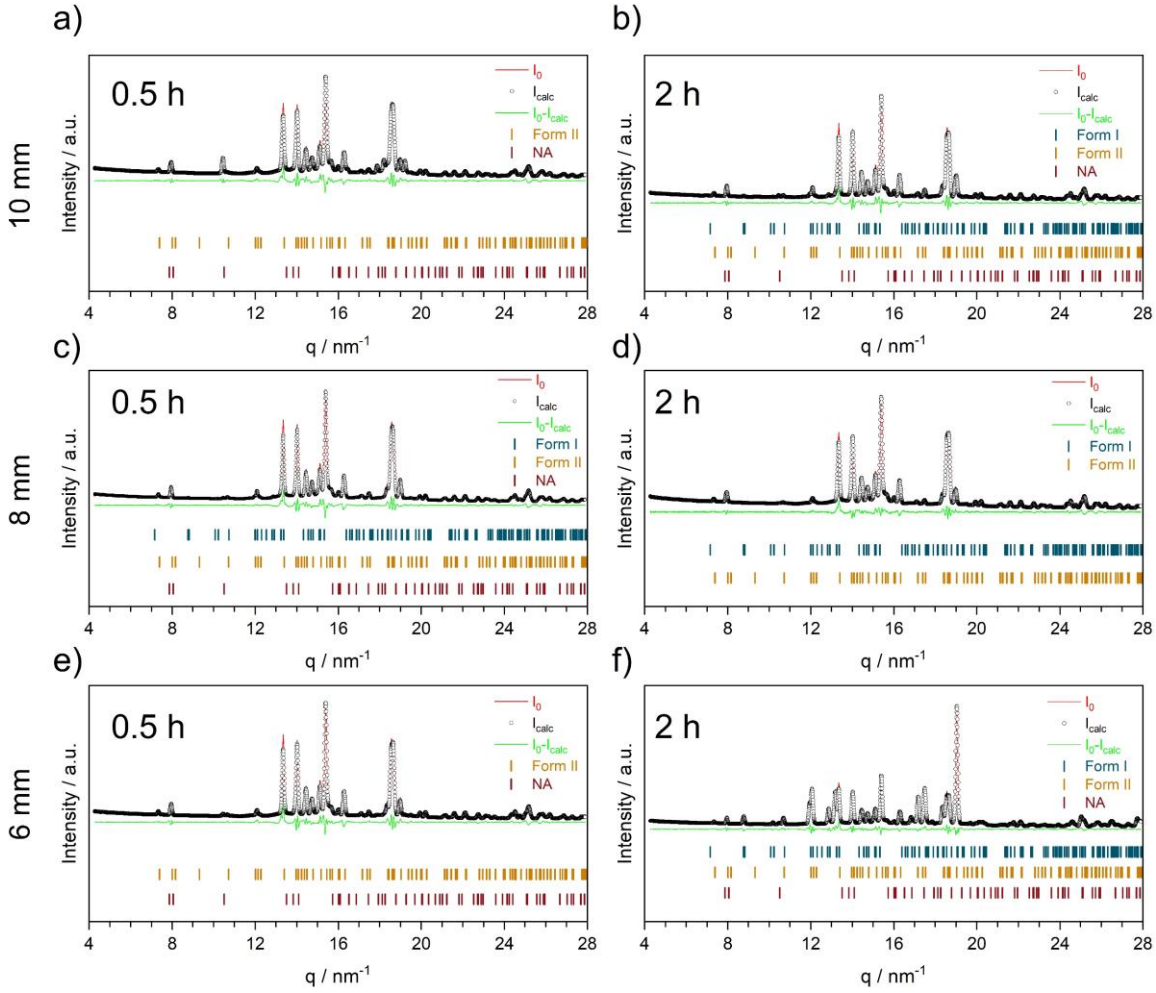

Figure S3.20| Results of the phase analyses for the mechanochemical synthesis of the cocrystal NA:PA with three different ball size (10, 8 and 6 mm) and a frequency of 35 Hz at 80°C: ball milling with a ball size of 10 mm (a: ball milling time of 0.5 h (R_{wp} = 7.213) and b: ball milling time of 2 h (R_{wp} = 7.667)); ball milling with a ball size of 8 mm (c: ball milling time of 0.5 h (R_{wp} = 7.413) and d: ball milling time of 2 h (R_{wp} = 6.368); ball milling with a ball size of 6 mm(e: ball milling time of 0.5 h (R_{wp} = 7.213) and f: ball milling time of 2 h (R_{wp} = 7.213).

Table S3.20| Results of the Rietveld quantitative phase analyses for the mechanochemical synthesis of the cocrystal NA:PA using three different ball sizes (10, 8 and 6 mm) and at a frequency of 35 Hz at 80°C.

Ball size	***time***	**Reagents /%**	**Form I / %**	**Form II / %**	**R_{wp}**
10	0.5 h	9	0	91	7.213
	2 h	1	7	92	7.667
8	0.5 h	1	3	96	7.413
	2 h	0	0	100	6.368
6	0.5 h	1	0	99	7.213
	2 h	1	61	38	7.213

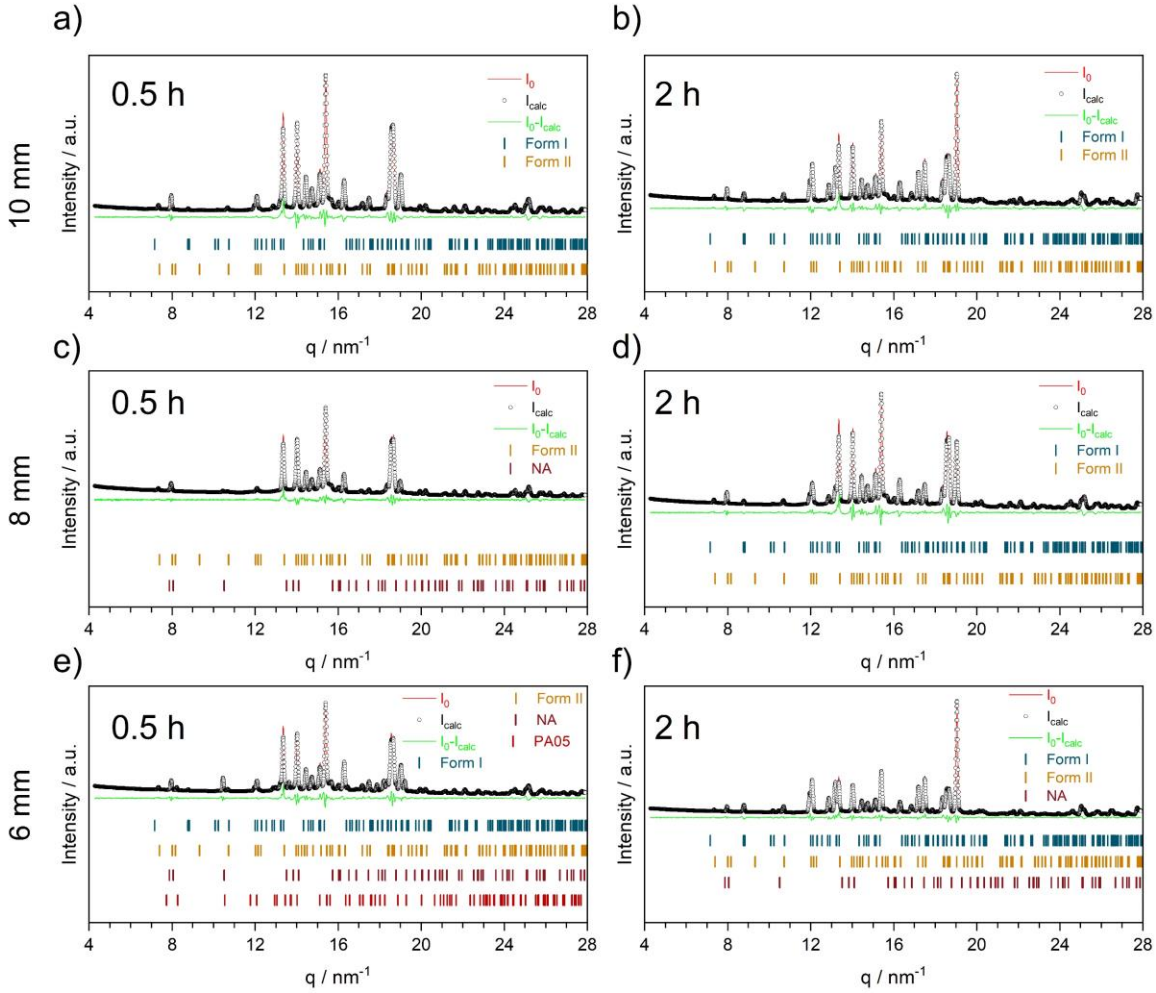

Figure S3.21| Results of the phase analyses for the mechanochemical synthesis of the cocrystal NA:PA with three different ball size (10, 8 and 6 mm) and a frequency of 20 Hz at 80°C: ball milling with a ball size of 10 mm (a: ball milling time of 0.5 h (R_{wp} = 7.283) and b: ball milling time of 2 h (R_{wp} = 7.147)); ball milling with a ball size of 8 mm (c: ball milling time of 0.5 h (R_{wp} = 6.639) and d: ball milling time of 2 h (R_{wp} = 7.147); ball milling with a ball size of 6 mm(e: ball milling time of 0.5 h (R_{wp} = 6.667) and f: ball milling time of 2 h (R_{wp} = 5.936).

Table S3.21| Results of the Rietveld quantitative phase analyses for the mechanochemical synthesis of the cocrystal NA:PA using three different ball sizes (10, 8 and 6 mm) and at a frequency of 20 Hz at 80°C.

Ball size	***time***	**Reagents /%**	**Form I / %**	**Form II / %**	**R_{wp}**
10	0.5 h	0	10	90	7.283
	2 h	0	47	53	7.147
8	0.5 h	1	0	99	6.639
	2 h	0	25	75	7.147
6	0.5 h	11	11	78	6.667
	2 h	1	62	37	5.936

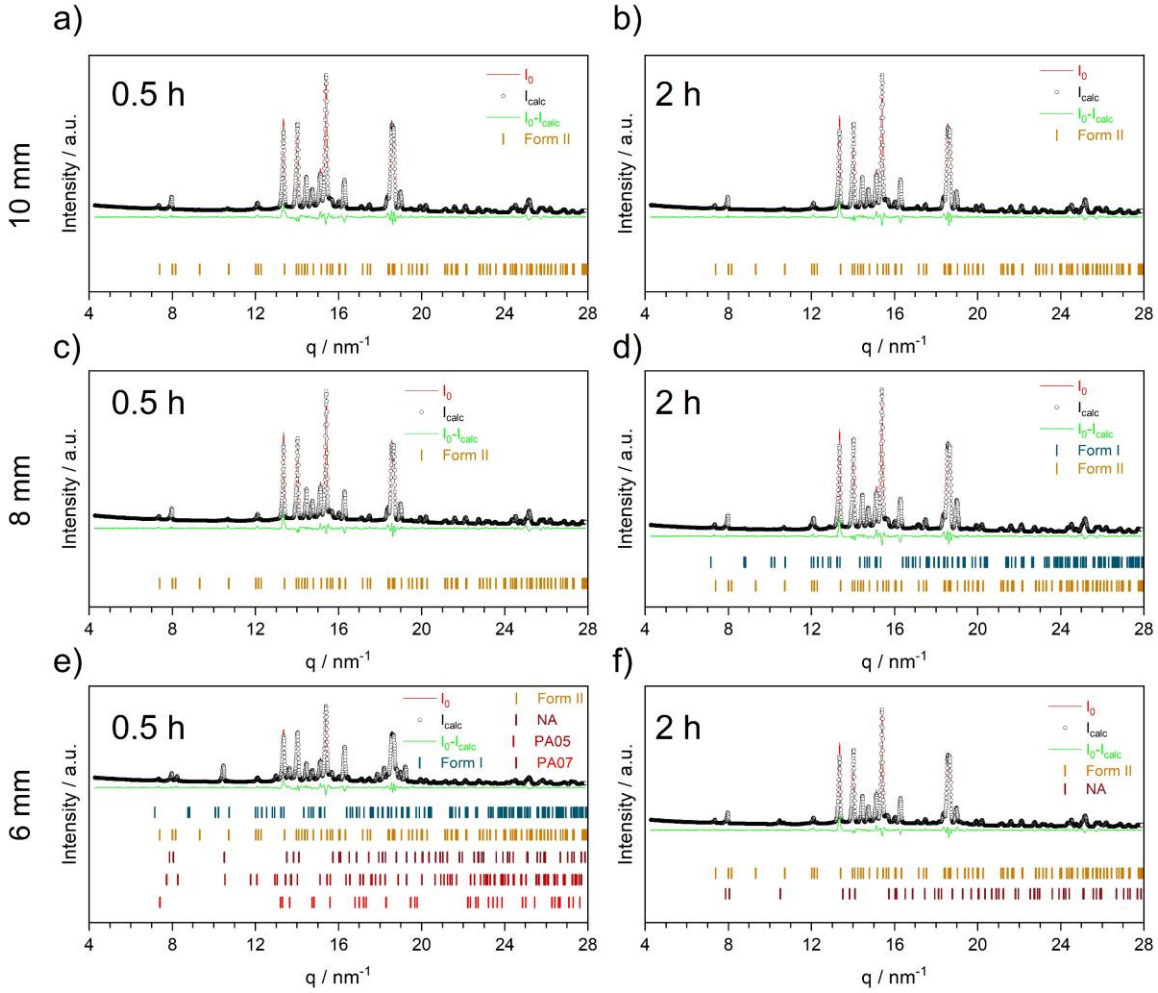

Figure S3.22| Results of the phase analyses for the mechanochemical synthesis of the cocrystal NA:PA with three different ball size (10, 8 and 6 mm) and a frequency of 20 Hz at 85°C: ball milling with a ball size of 10 mm (a: ball milling time of 0.5 h (R_{wp} = 6.434) and b: ball milling time of 2 h (R_{wp} = 6.534)); ball milling with a ball size of 8 mm (c: ball milling time of 0.5 h (R_{wp} = 6.314) and d: ball milling time of 2 h (R_{wp} = 6.629); ball milling with a ball size of 6 mm(e: ball milling time of 0.5 h (R_{wp} = 5.718) and f: ball milling time of 2 h (R_{wp} = 6.464).

Table S3.22| Results of the Rietveld quantitative phase analyses for the mechanochemical synthesis of the cocrystal NA:PA using three different ball sizes (10, 8 and 6 mm) and at a frequency of 50 Hz at 85°C.

Ball size	***time***	**Reagents /%**	**Form I / %**	**Form II / %**	**R_{wp}**
10	0.5 h	0	0	100	6.434
	2 h	0	0	100	6.534
8	0.5 h	0	0	100	6.314
	2 h	0	7	93	6.629
6	0.5 h	22	2	76	5.718
	2 h	2	0	98	6.464

5. References

(1) Aitipamula, S.; Wong, A. B. H.; Chow, P. S.; Tan, R. B. H. Polymorphism and Phase Transformations of a Cocrystal of Nicotinamide and Pimelic Acid. *CrystEngComm* **2012**, *14* (23), 8193–8198. https://doi.org/10.1039/C2CE26151K.

(2) Lampronti, G. I.; Michalchuk, A. A.; Mazzeo, P. P. Changing the Game of Time Resolved X-Ray Diffraction on the Mechanochemistry Playground by Downsizing.

(3) Linberg, K.; Röder, B.; Al-Sabbagh, D.; Emmerling, F.; Michalchuk, A. A. L. Controlling Polymorphism in Molecular Cocrystals by Variable Temperature Ball Milling. *Faraday Discuss.* **2022**. https://doi.org/10.1039/D2FD00115B.

(4) Bruker, A. Topas V4. 2: General Profile and Structure Analysis Software for Powder Diffraction Data. *Bruker AXS, Karlsruhe, Germany* **2009**.

(5) Lemmerer, A.; Adsmond, D. A.; Esterhuysen, C.; Bernstein, J. Polymorphic Co-Crystals from Polymorphic Co-Crystal Formers: Competition between Carboxylic Acid···Pyridine and Phenol···Pyridine Hydrogen Bonds. *Crystal Growth & Design* **2013**, *13* (9), 3935–3952. https://doi.org/10.1021/cg4006357.

(6) Wright, W. B.; King, G. S. D. The Crystal Structure of Nicotinamide. *Acta Crystallographica* **1954**, *7* (3), 283–288.

(7) Thalladi, V. R.; Nüsse, M.; Boese, R. The Melting Point Alternation in α,ω-Alkanedicarboxylic Acids. *J. Am. Chem. Soc.* **2000**, *122* (38), 9227–9236. https://doi.org/10.1021/ja0011459.

(8) Mitchell, C. A.; Yu, L.; Ward, M. D. Selective Nucleation and Discovery of Organic Polymorphs through Epitaxy with Single Crystal Substrates. *J. Am. Chem. Soc.* **2001**, *123* (44), 10830–10839. https://doi.org/10.1021/ja004085f.

(9) Michalchuk, A. A.; Emmerling, F. Time-Resolved In Situ Monitoring of Mechanochemical Reactions. *Angewandte Chemie* **2022**.

(10) Zizak, I. MySpot: A Versatile Microfocussing Station for Scanning Methods at BESSY II. *Journal of large-scale research facilities JLSRF* **2016**, *2*, A101–A101.

(11) Benecke, G.; Wagermaier, W.; Li, C.; Schwartzkopf, M.; Flucke, G.; Hoerth, R.; Zizak, I.; Burghammer, M.; Metwalli, E.; Muller-Buschbaum, P.; Trebbin, M.; Forster, S.; Paris, O.; Roth, S. V.; Fratzl, P. A Customizable Software for Fast Reduction and Analysis of Large X-Ray Scattering Data Sets: Applications of the New DPDAK Package to Small-Angle X-Ray Scattering and Grazing-Incidence Small-Angle X-Ray Scattering. *Journal of Applied Crystallography*, 2014, *47*, 1797–1803. https://doi.org/doi:10.1107/S1600576714019773.

(12) Baek, S.-J.; Park, A.; Ahn, Y.-J.; Choo, J. Baseline Correction Using Asymmetrically Reweighted Penalized Least Squares Smoothing. *Analyst* **2015**, *140* (1), 250–257. https://doi.org/10.1039/C4AN01061B.

(13) Clark, S. J.; Segall, M. D.; Pickard, C. J.; Hasnip, P. J.; Probert, M. I.; Refson, K.; Payne, M. C. First Principles Methods Using CASTEP. *Zeitschrift für Kristallographie-Crystalline Materials* **2005**, *220* (5–6), 567–570.

(14) Ernzerhof, M.; Scuseria, G. E. Assessment of the Perdew–Burke–Ernzerhof Exchange-Correlation Functional. *The Journal of chemical physics* **1999**, *110* (11), 5029–5036.

(15) Tkatchenko, A.; Scheffler, M. Accurate Molecular van Der Waals Interactions from Ground-State Electron Density and Free-Atom Reference Data. *Physical review letters* **2009**, *102* (7), 073005.

(16) Refson, K.; Tulip, P. R.; Clark, S. J. Variational Density-Functional Perturbation Theory for Dielectrics and Lattice Dynamics. *Physical Review B* **2006**, *73* (15), 155114.